

Nucleosynthesis of trans-iron elements

Teresa Kurtukian-Nieto

LP2i Bordeaux/CNRS-IN2P3, Gradignan, France

Neutron Pathways to Nucleosynthesis

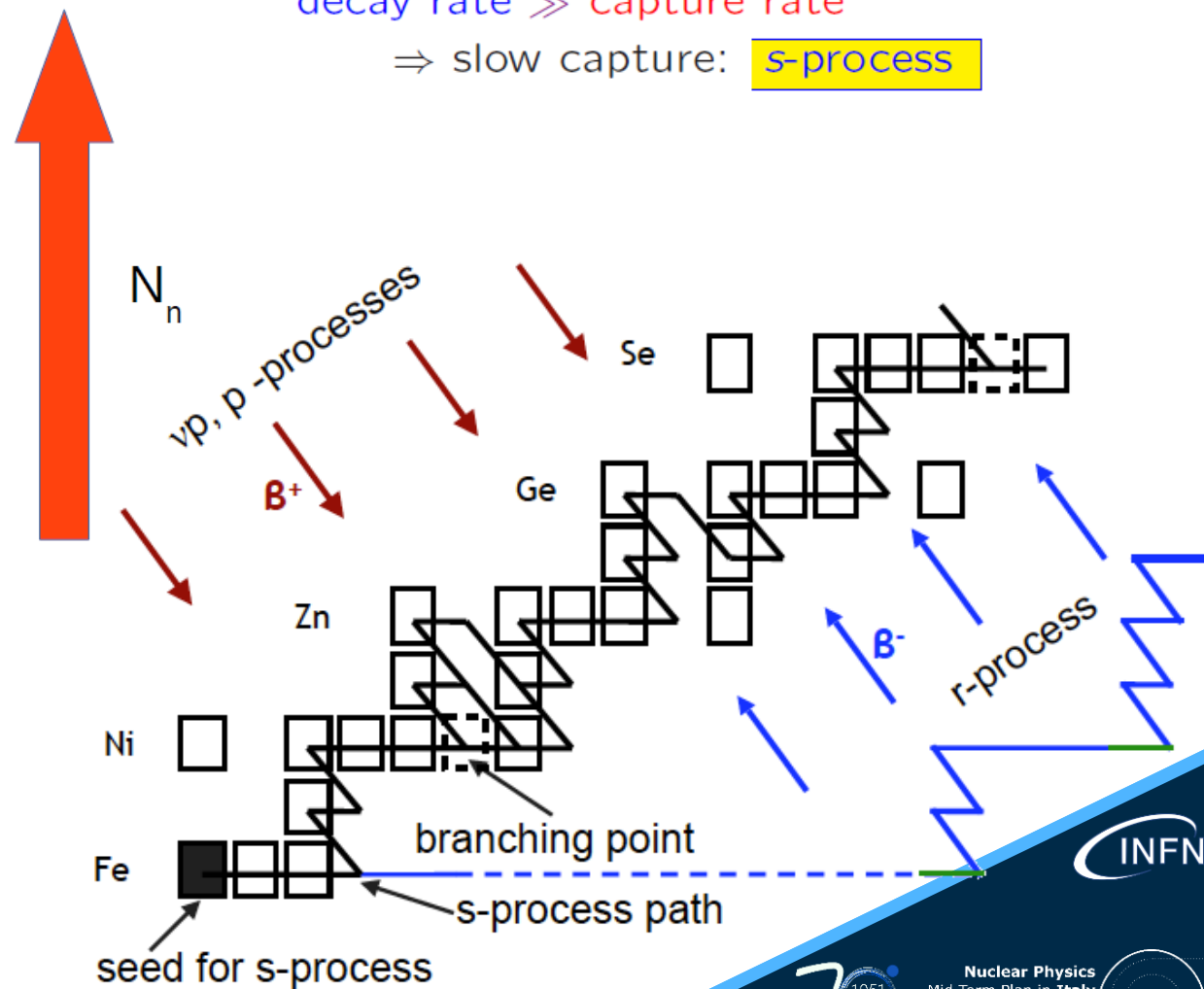
- ✓ **The r process**
(neutrino-wind, NS mergers, jet-SNe, etc)
 $N_n > 10^{20} \text{ n cm}^{-3}$;
- ✓ The n process
(explosive He-burning in CCSN)
 $10^{18} \text{ n cm}^{-3} < N_n < 10^{20} \text{ n cm}^{-3}$;
- ✓ The i process
(H ingestion in convective He burning conditions)
 $10^{14} \text{ n cm}^{-3} < N_n < 10^{16} \text{ n cm}^{-3}$;
- ✓ Neutron capture triggered by the $^{22}\text{Ne}(\alpha, n)^{25}\text{Mg}$ in massive AGB stars and super-AGB stars
 $N_n < 10^{14} \text{ n cm}^{-3}$;
- ✓ **The s process**
(s process in AGB stars, s process in massive stars and fast rotators)
 $N_n < \text{few } 10^{12} \text{ n cm}^{-3}$.

capture rate \gg decay rate

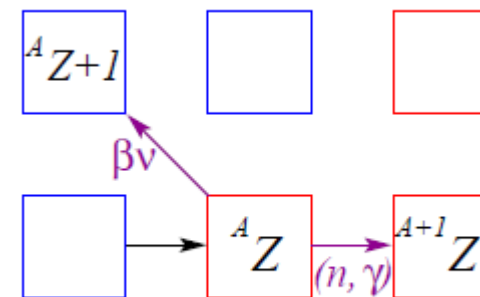
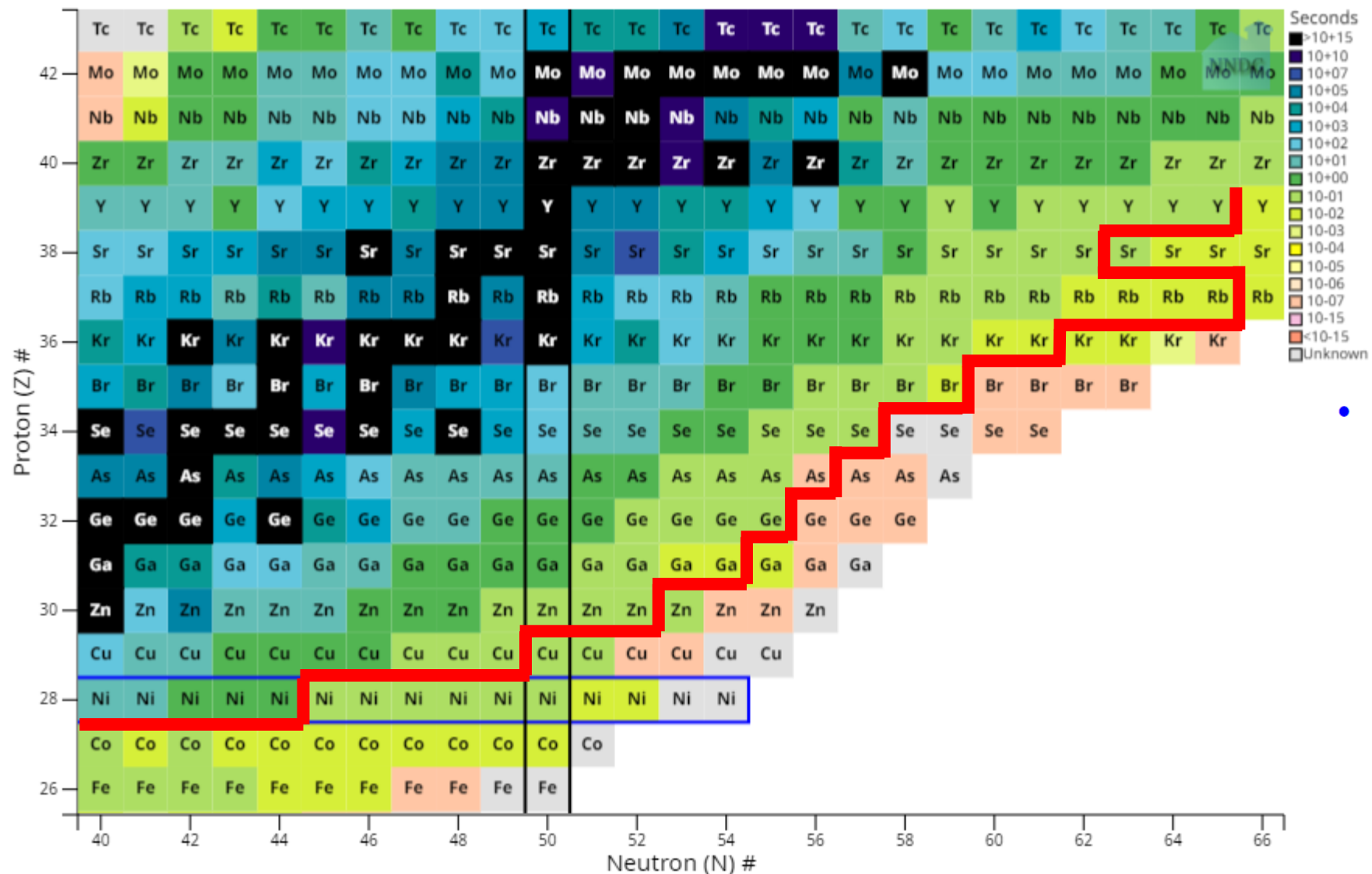
\Rightarrow rapid capture: **r-process**

decay rate \gg capture rate

\Rightarrow slow capture: **s-process**

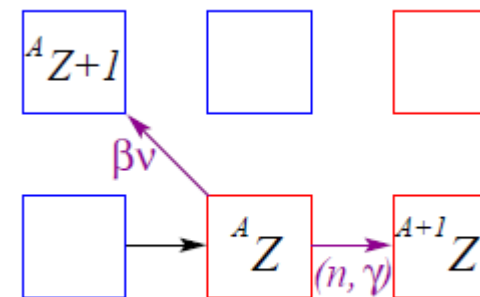
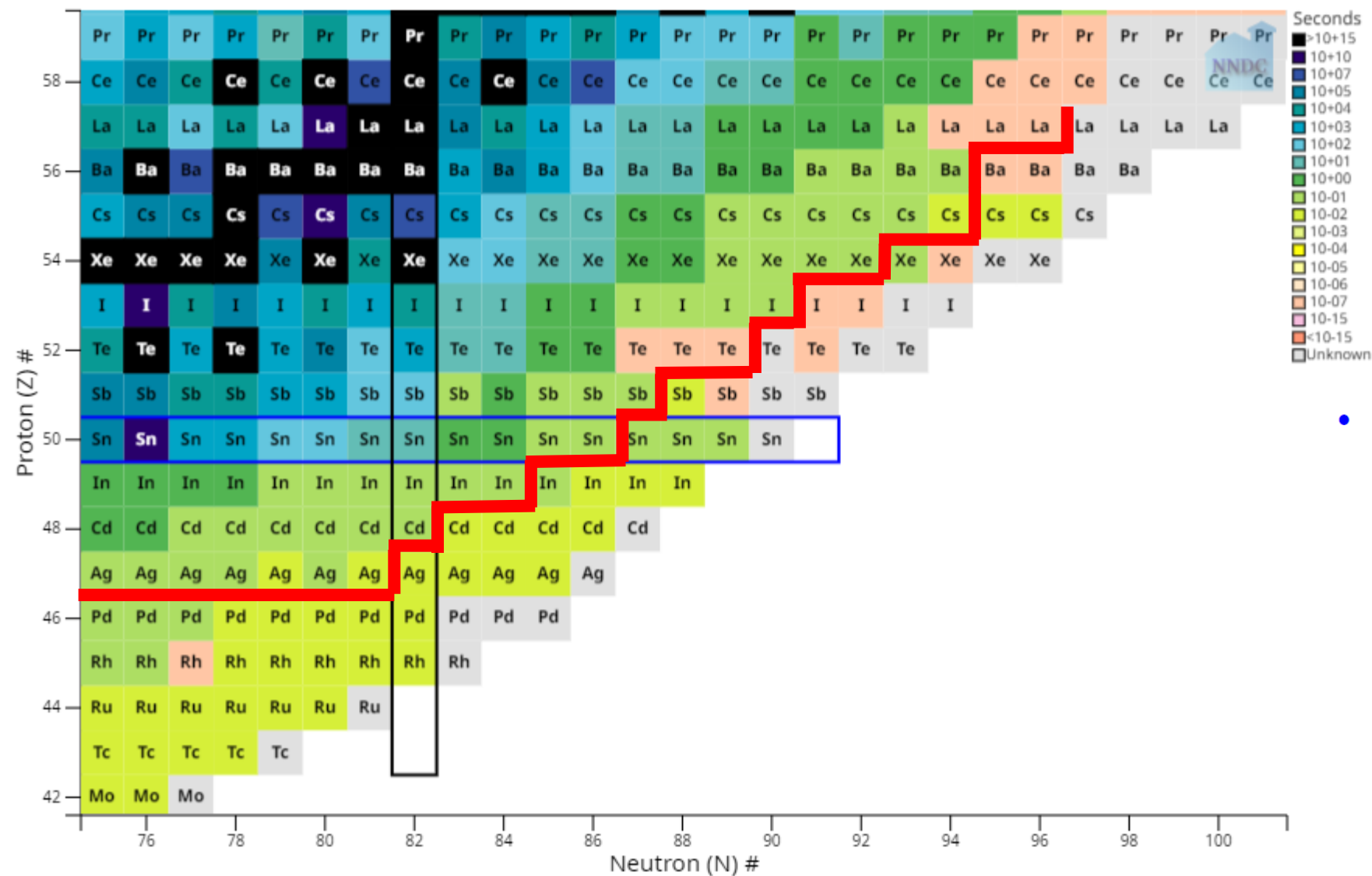


Experimental nuclear data at 1st peak



- beta decay rates ^{89}As

Experimental nuclear data at 2nd peak

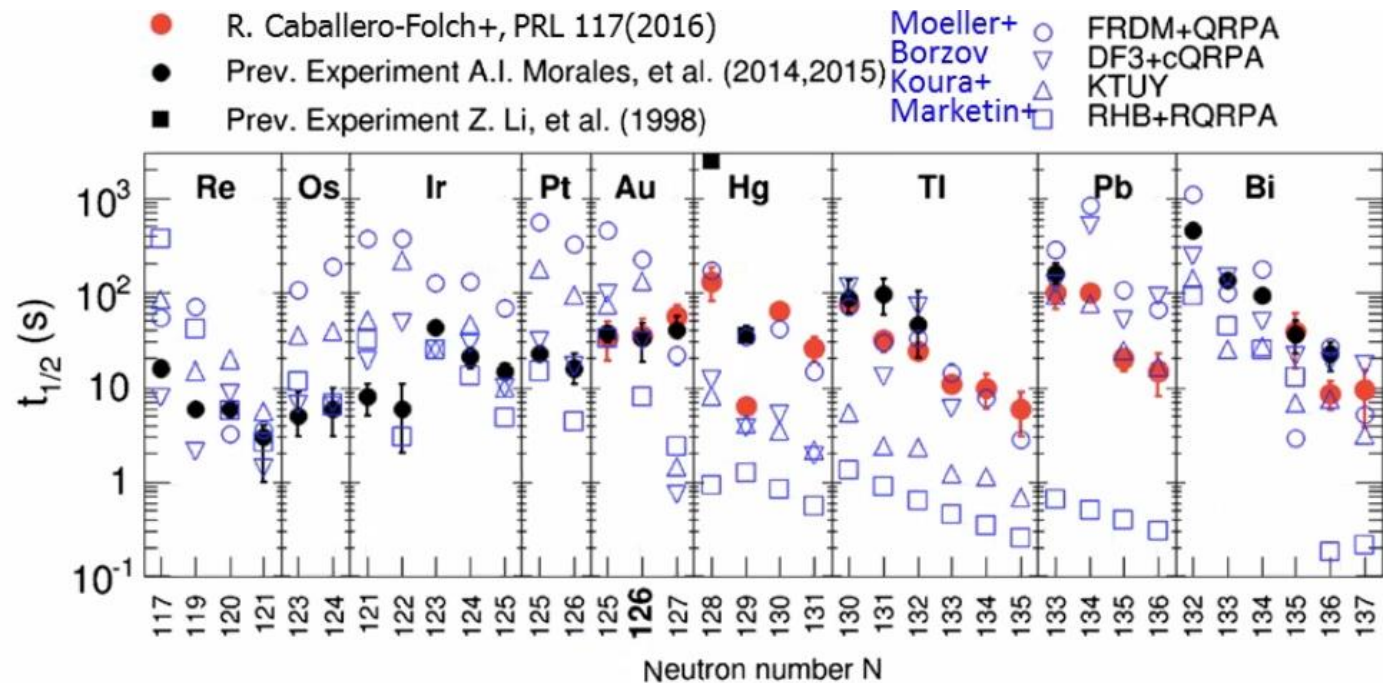
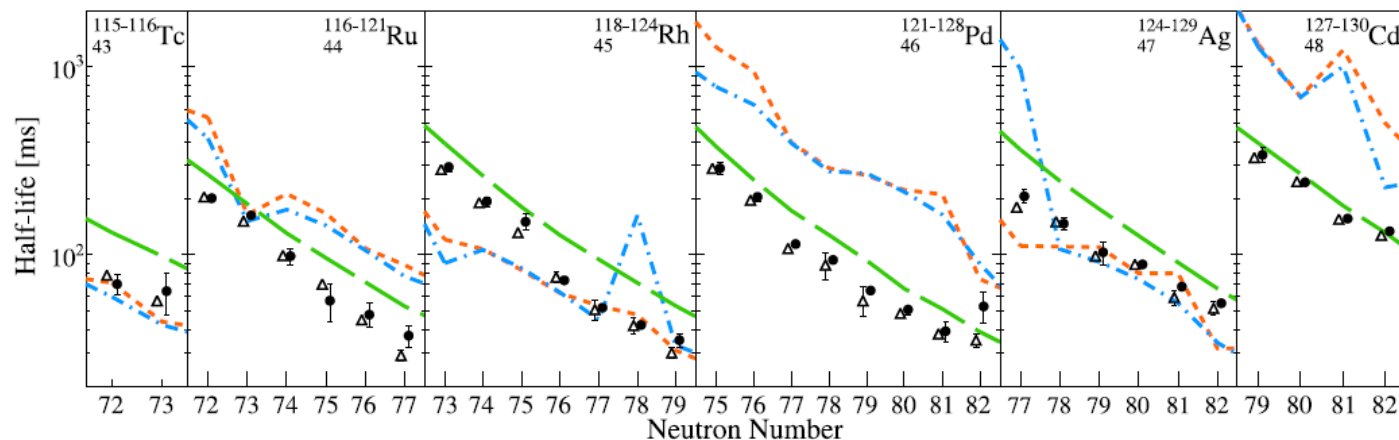


- beta decay rates $^{151-153}\text{La}$
 $^{139-141}\text{Te}$

How good are models?

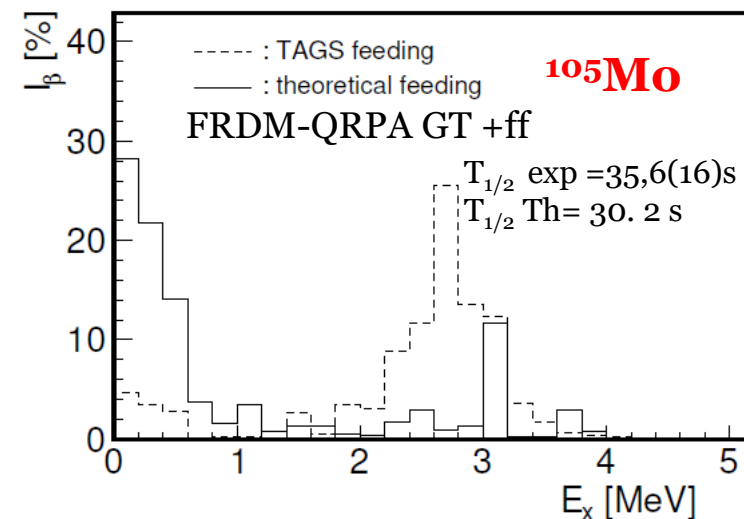
O. Hall et al., Physics Letters B, 816, 136266 (2021)

- This work Δ Lorusso et al. - - - FRDM+QRPA - - - FRDM+QRPA+HF — RHB+pn-RQRPA



$$\frac{1}{T_{1/2}} = \int_0^{Q_\beta} S_\beta(E) f(Q_\beta - E) dE$$

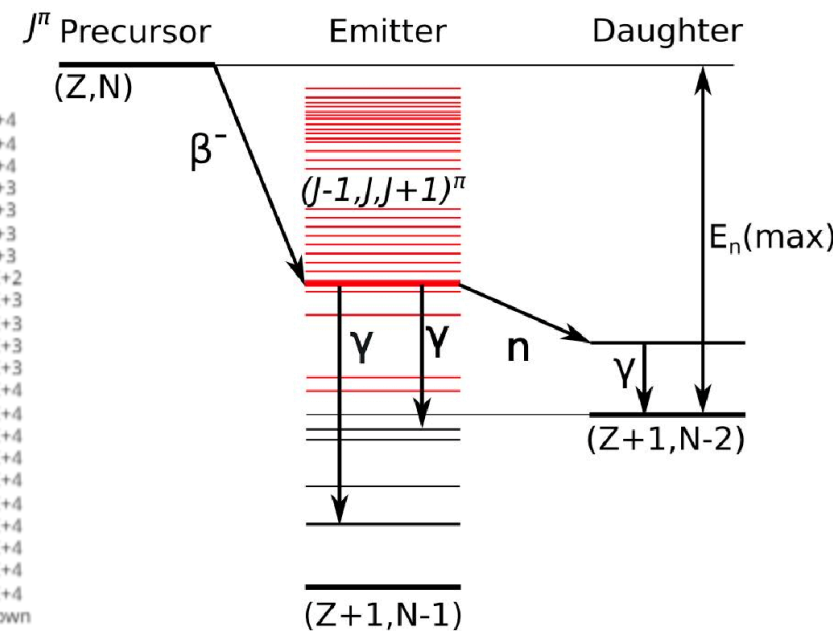
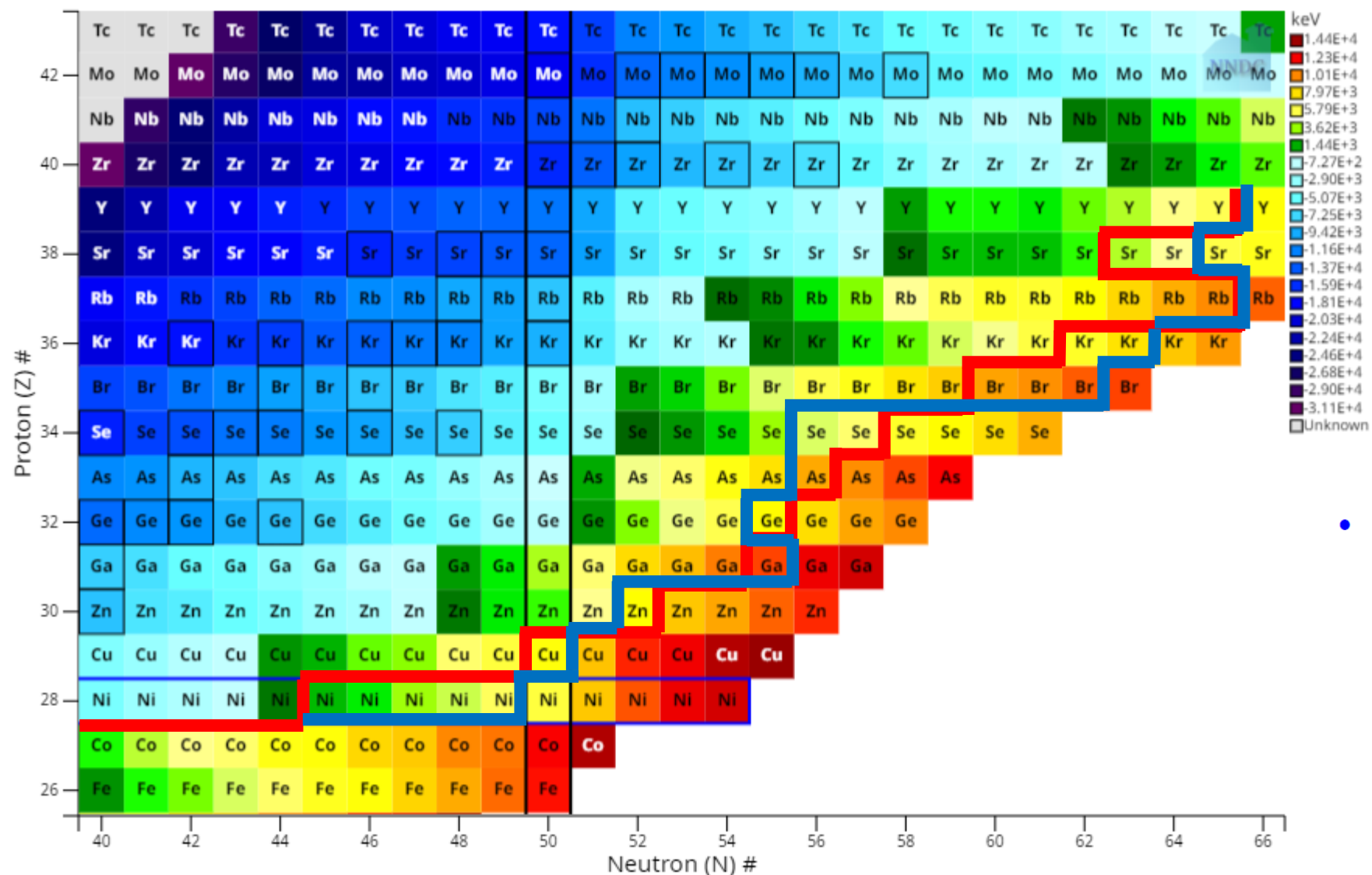
$$S_\beta(E) = \frac{I_\beta(E)}{f(Q_\beta - E) T_{1/2}}$$



A. Algora et al.,

$$P_n = T_{1/2} \int_{S_n}^{Q_\beta} \frac{\Gamma_n}{\Gamma_n + \Gamma_\gamma} S_\beta(E) f(Q_\beta - E) dE$$

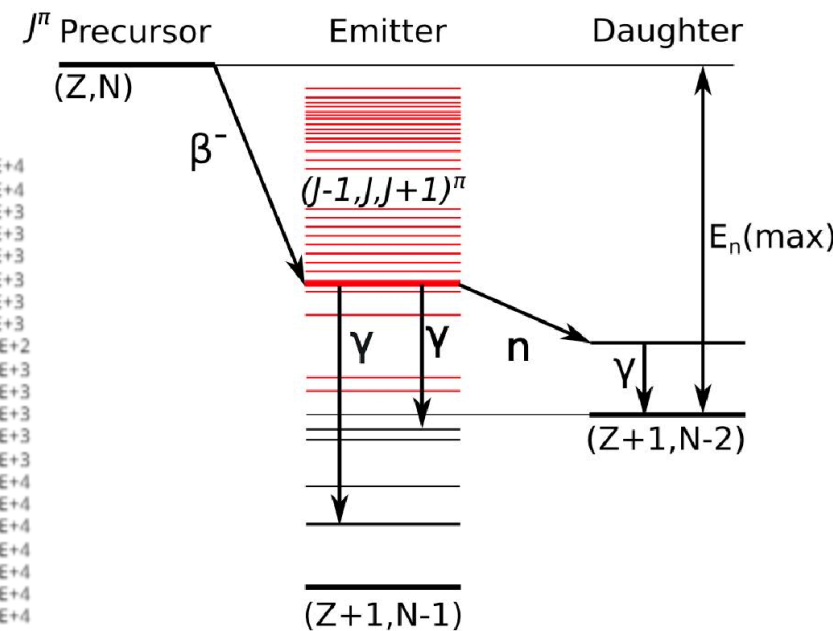
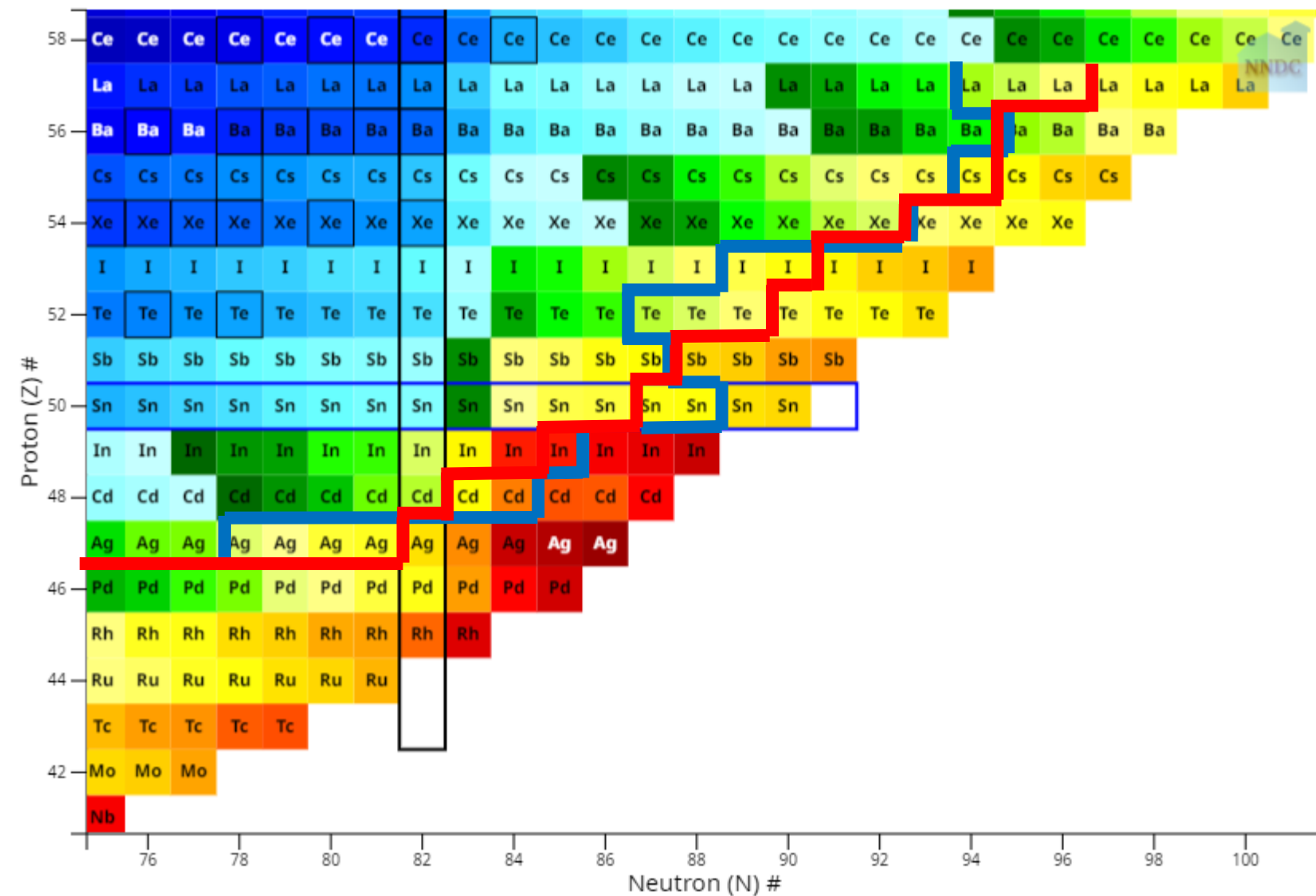
Experimental nuclear data at 1st peak



- Beta-delayed neutron emission

^{82}Zn , ^{87}Ge , ^{89}As , ^{90}Se

Experimental nuclear data at 2nd peak



- Beta-delayed neutron emission

$^{151-153}\text{La}$

^{148}Cs

$^{142-143}\text{I}$

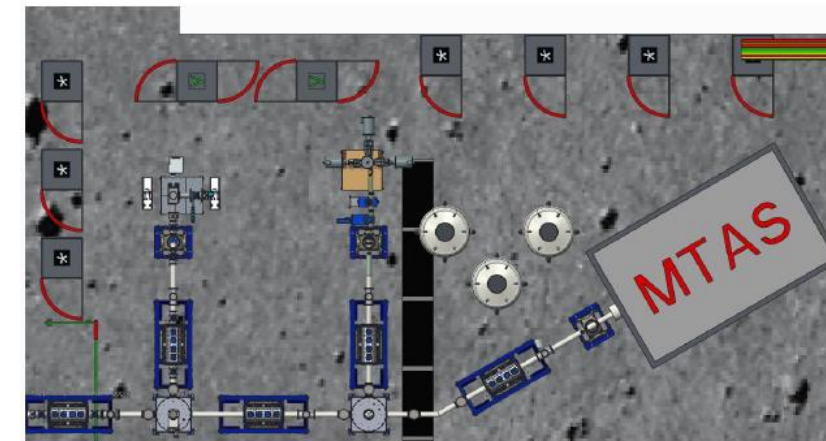
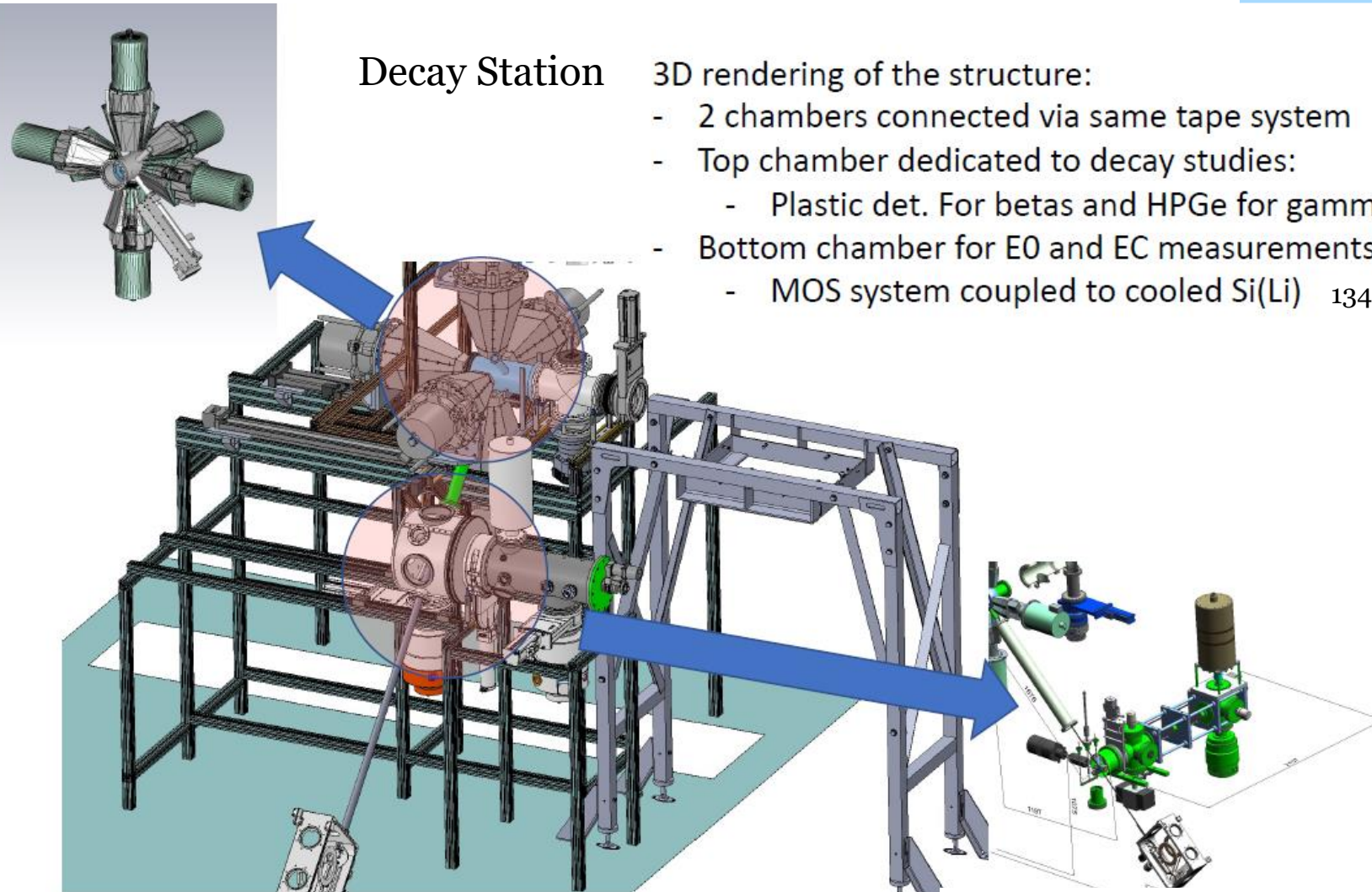
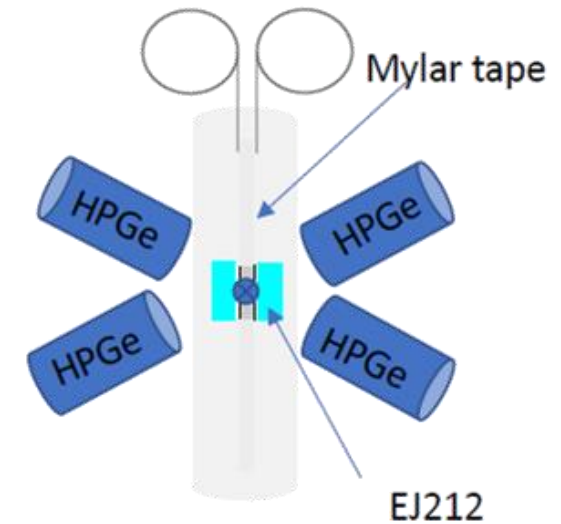
$^{139-141}\text{Te}$

$^{125-128}\text{Ag}$

Decay Station

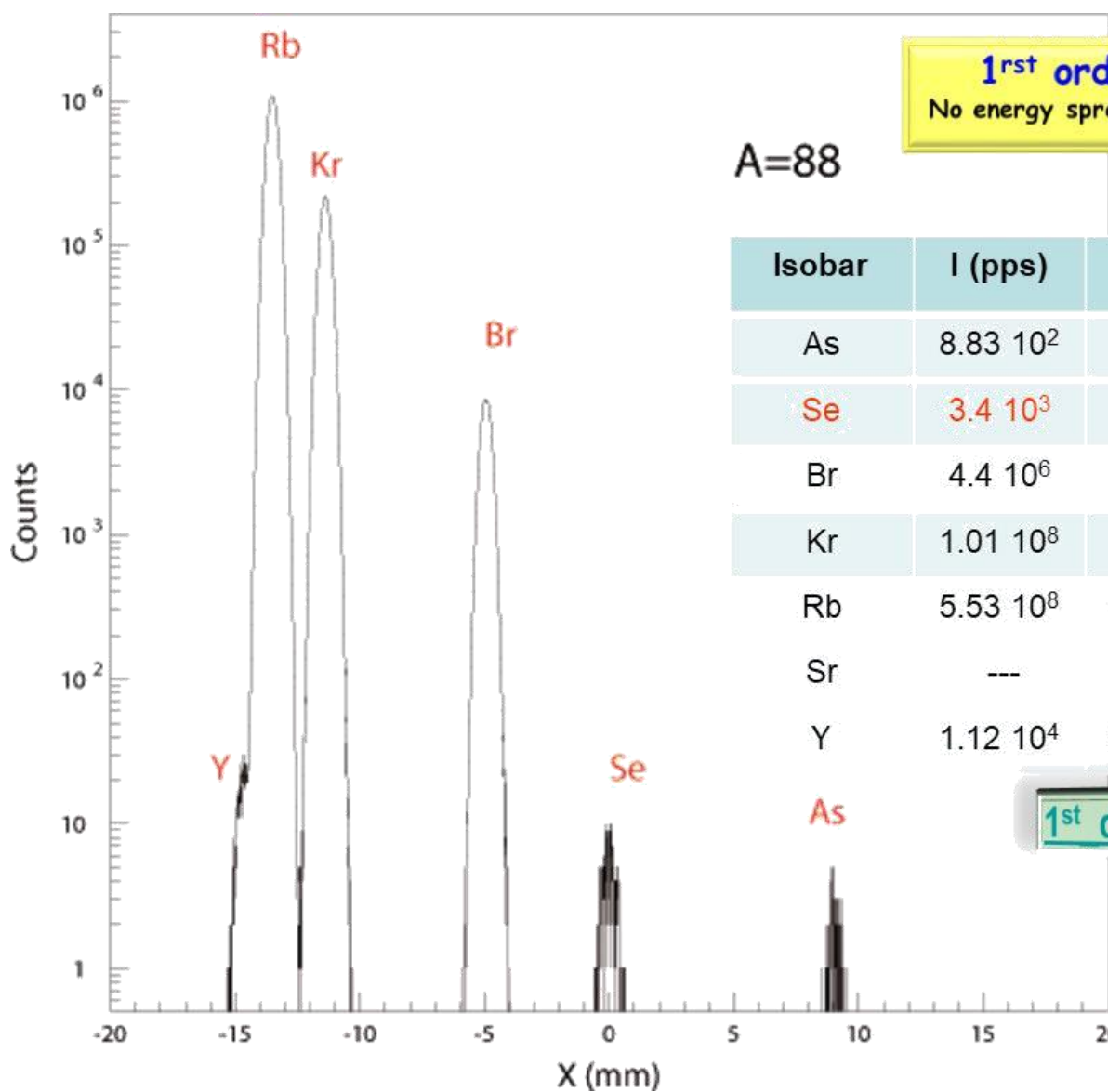
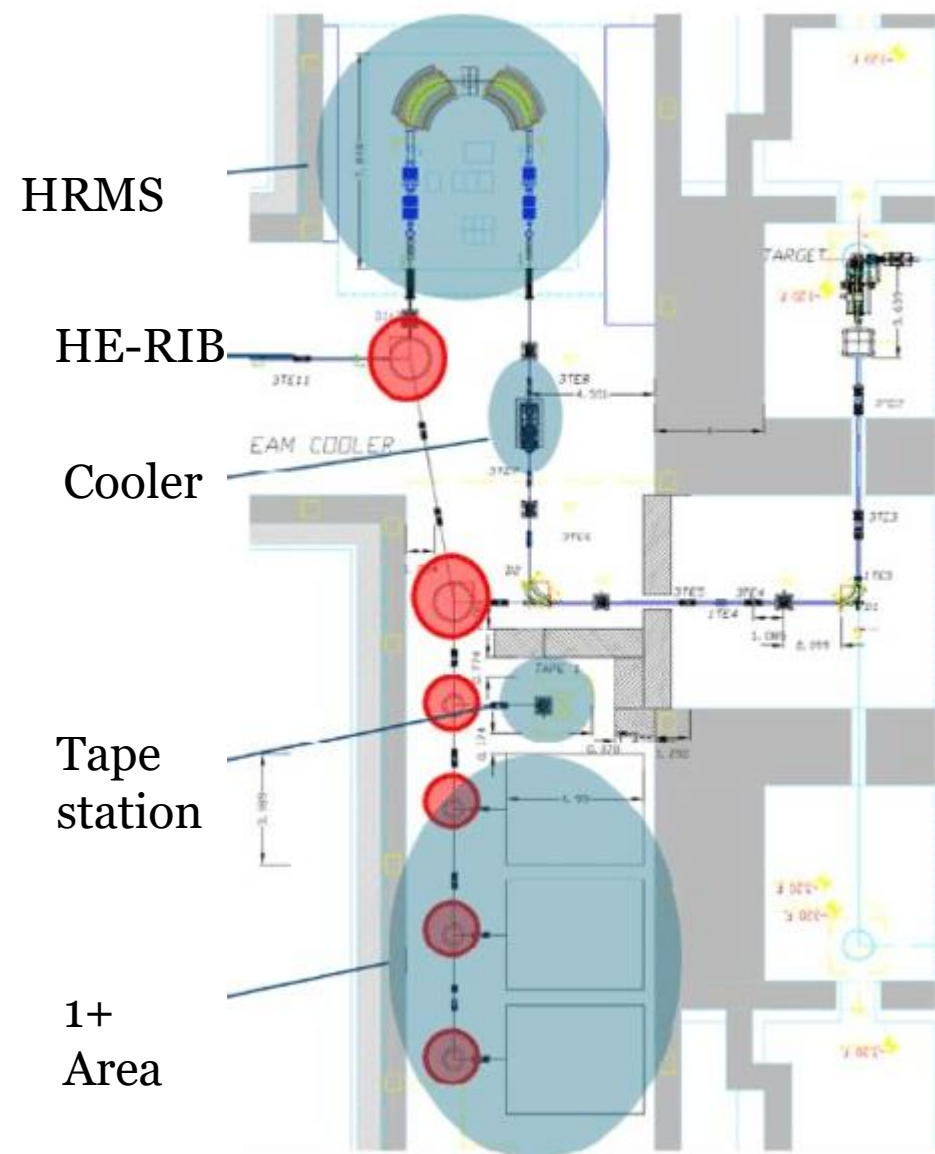
3D rendering of the structure:

- 2 chambers connected via same tape system
- Top chamber dedicated to decay studies:
 - Plastic det. For betas and HPGe for gammas
- Bottom chamber for E0 and EC measurements:
 - MOS system coupled to cooled Si(Li) ^{134}Cs



- Implantation and decay in the same measuring point
- Equipped with HPGe for γ and Plastic (or Si) for β particles
- Trigger given by proton arrival and β signal
- Long-living activity is removed by moving away the tape

Use of SPES HRMS for isobar purification



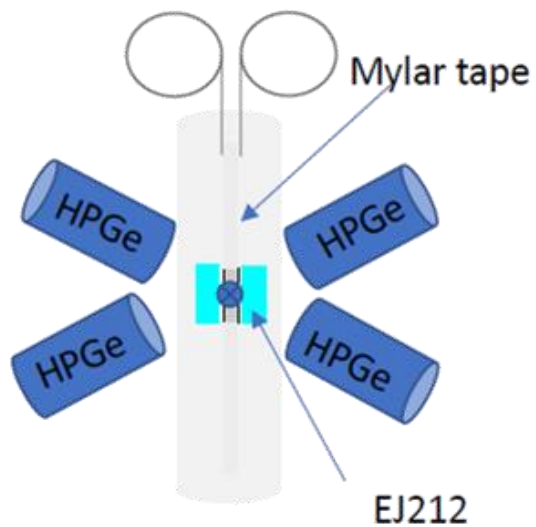
1st order calculation:
No energy spread/misalignment included

A=88

| Isobar | I (pps) | T _{1/2} | m/Δm |
|--------|------------------------|------------------|---------|
| As | 8.83 · 10 ² | | -6 511 |
| Se | 3.4 · 10 ³ | 1.53 (6) s | 0 |
| Br | 4.4 · 10 ⁶ | 16.29(6) s | +11 960 |
| Kr | 1.01 · 10 ⁸ | 2.84 (3) h | +5 184 |
| Rb | 5.53 · 10 ⁸ | 17.773(11) m | +4 376 |
| Sr | --- | stable | +3409 |
| Y | 1.12 · 10 ⁴ | 106.626(21) d | +4 014 |

1st day UCx 5μA

Measurement of the decay characteristics



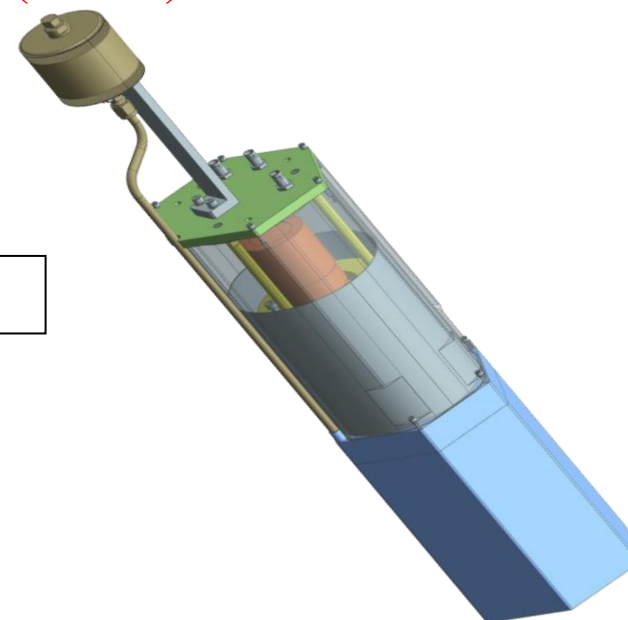
Tape transport system
Beam-on/off time sequence
 β - γ , γ - γ coincidence for β decay studies

detection

- β plastic scintillator
- γ germanium

Can be coupled with a neutron-detector (NEDA)

- ✓ Pn of the nuclei of interest.
- ✓ neutron-gated γ -ray spectra



Accumulation

Measuring time

Transport

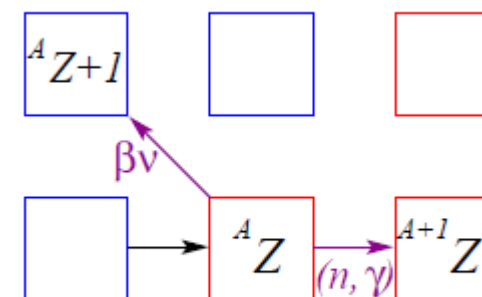
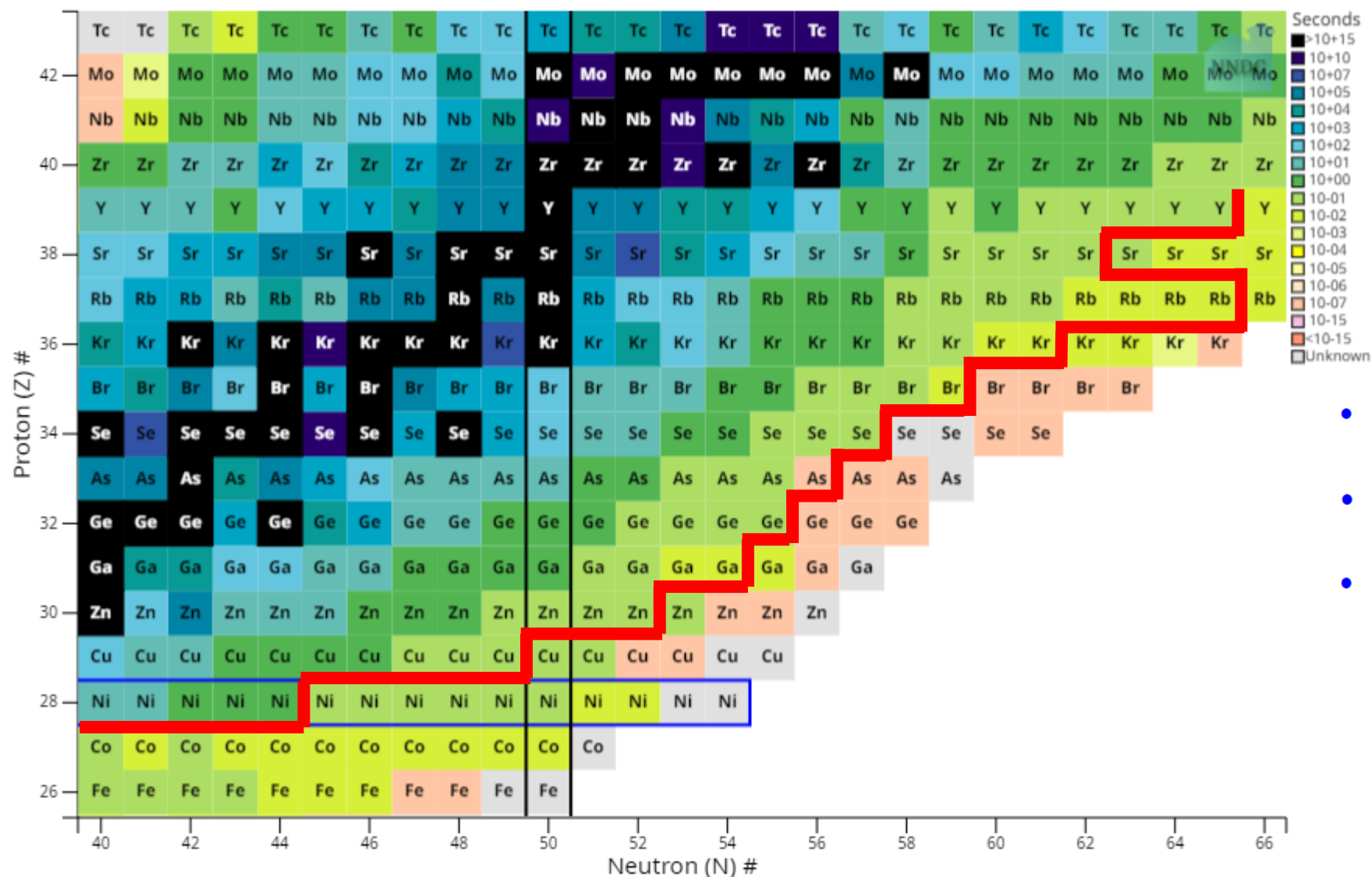
• cycle length:

- Half-lives
- BR

$$1T_{1/2} + 5 T_{1/2} + T_t$$

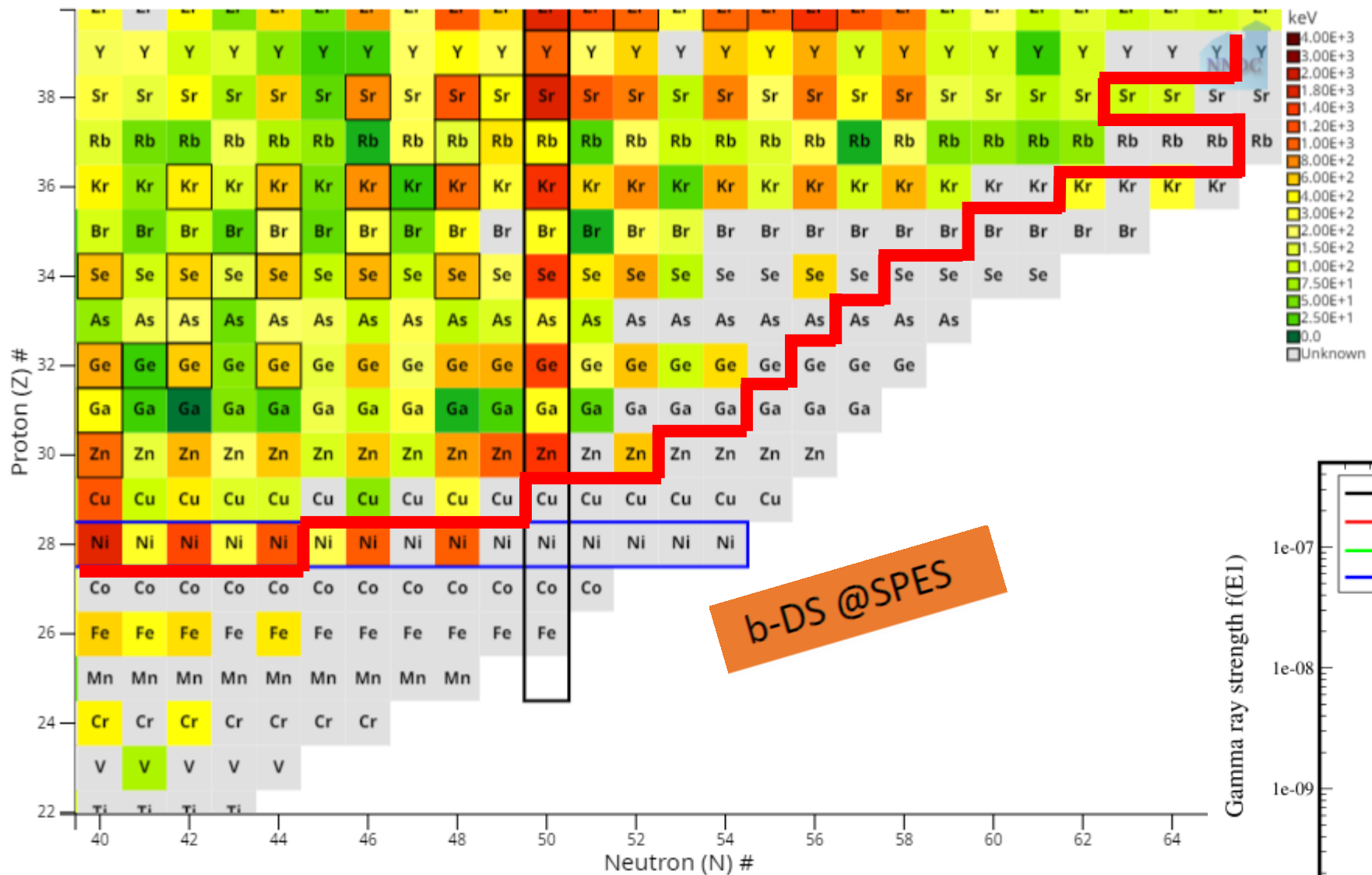
$$1T_{1/2} + 3T_{1/2} + T_t$$

Experimental nuclear data



- beta decay rates
- Beta-delayed neutron emission
- neutron capture rates

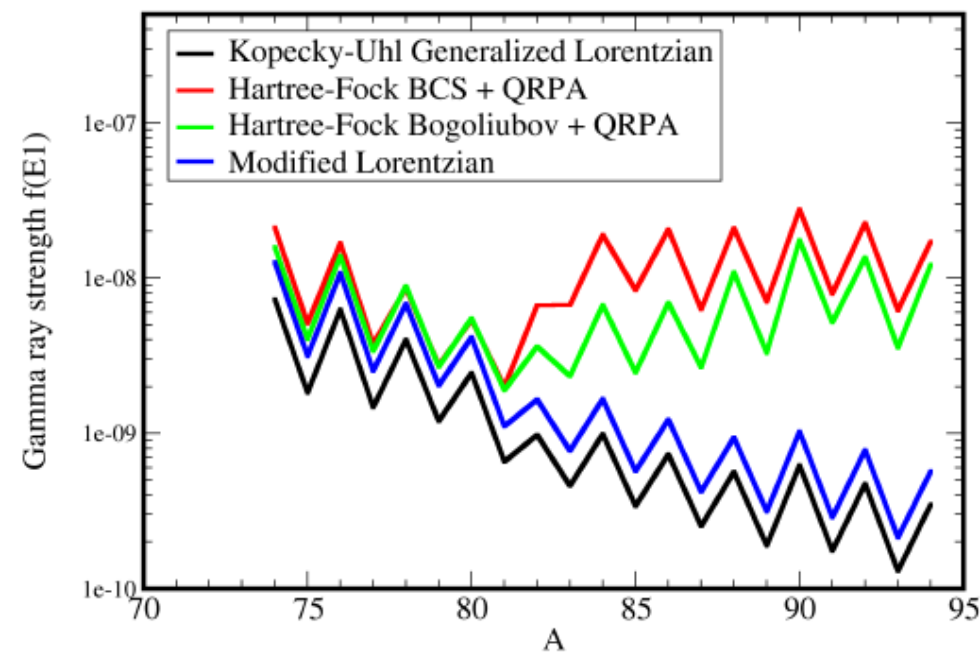
Decay schemes for (n,γ) cross-sections



Gamma ray emission in the Hauser-Feshbach model is described by the gamma-ray transmission coefficient.

$$T_l = 2\pi f_l(E_\gamma) E_\gamma^{2l+1}$$

S. Nikas et al.,
<https://arxiv.org/abs/2010.01698>
 f(E1) strength for (n,γ) on Ga isotopes @ 1GK



Activation measurements of isotopes of interest for the s-process

Maxwellian Averaged Cross Section (MACS)

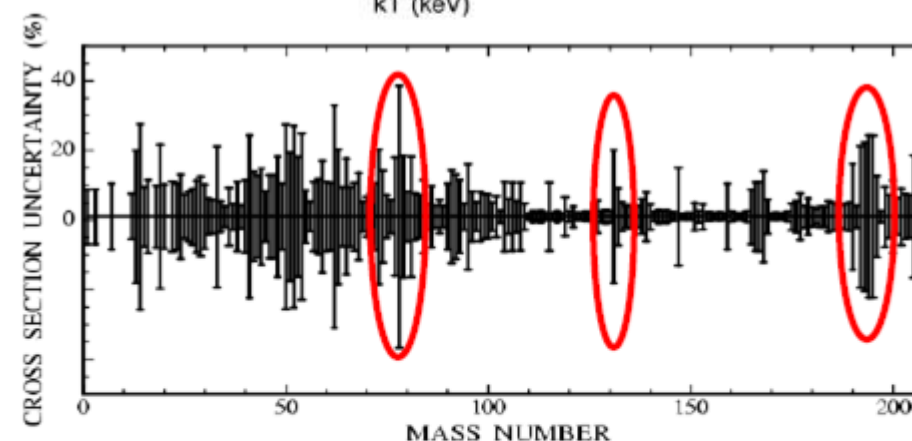
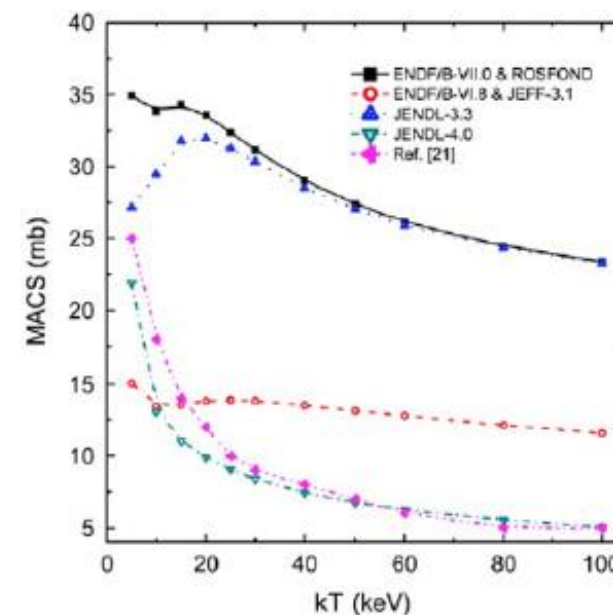
$$\text{MACS} = \langle \sigma \rangle = \frac{\langle \sigma v \rangle}{v_T} = \frac{2}{\sqrt{\pi}} \frac{1}{(kT)^2} \int_0^\infty \sigma(E) E \exp\left(-\frac{E}{kT}\right) dE$$

s-process reaction rate

$$\langle \sigma v \rangle = \int_0^\infty \Phi(v) \sigma(v) v dv = 4\pi \left(\frac{\mu}{2\pi kT}\right)^{3/2} \int_0^\infty \sigma(v) v^3 \exp\left(-\frac{\mu v^2}{kT}\right) dv$$

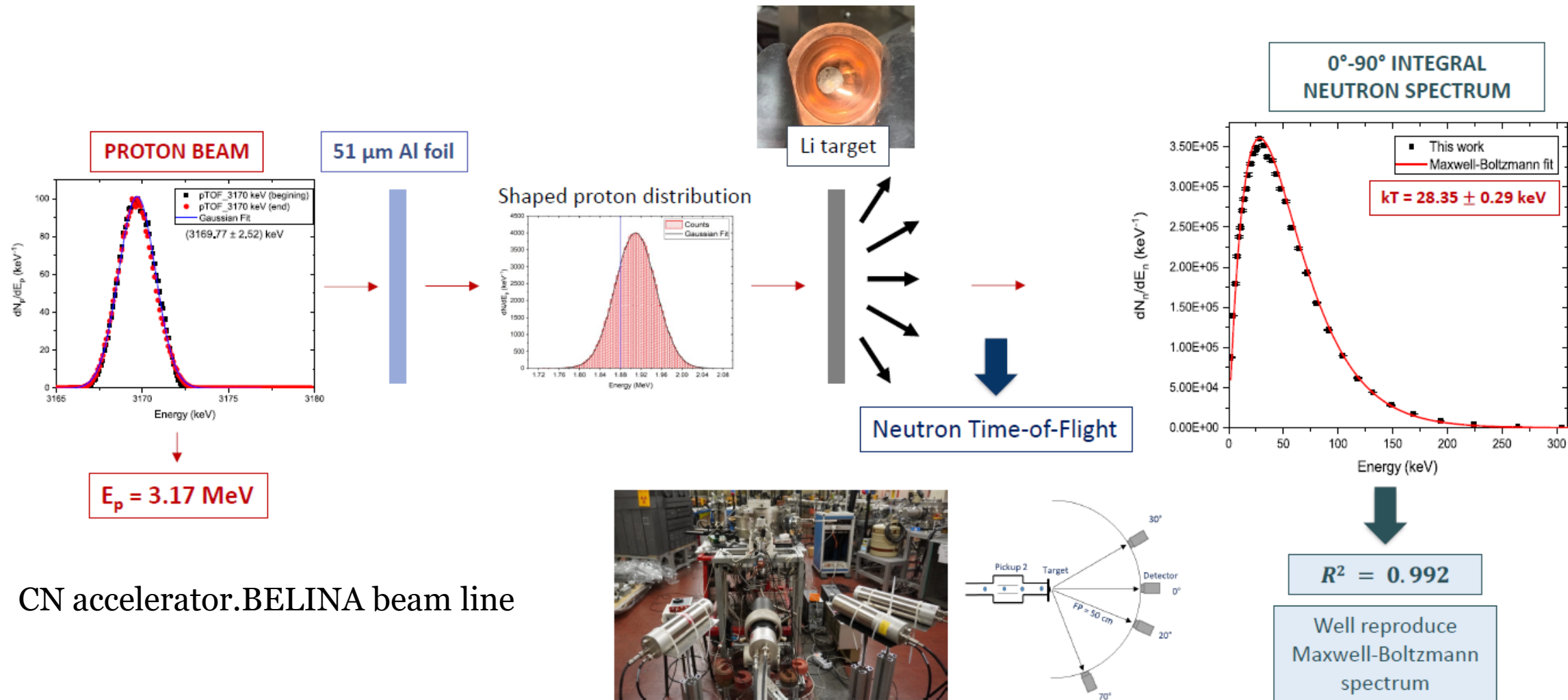
Predicted Abundance

Comparison with experimental observed abundances



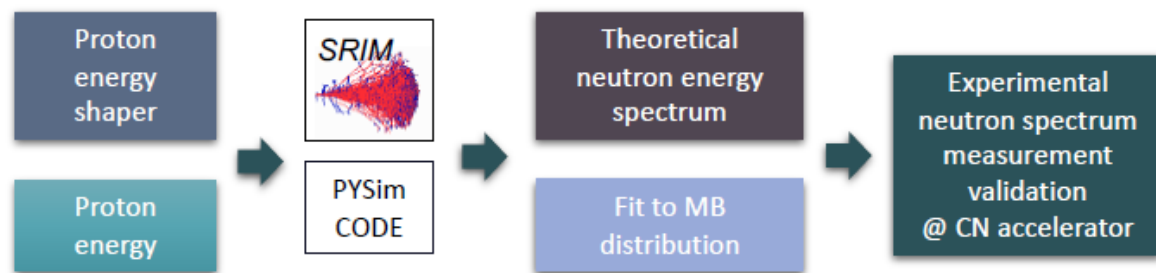
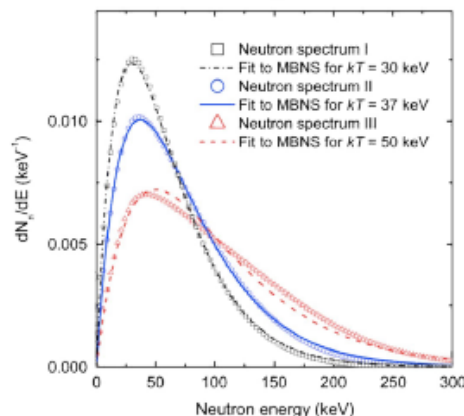
MACS calculated uncertainties of several stable and most of the unstable isotopes are higher than the requested accuracy (for s-process: 3-5%).

Activation measurements of isotopes of interest for the s-process



Activation measurements of isotopes of interest for the s-process

Produce and measure Maxwell-Boltzmann-like neutron spectrum at different kT



Case of study: ^{88}Sr

PHASE A

PHASE B irradiation of radioactive targets produced at SPES

Activation measurements to determine the MACS of isotopes of interest at different thermal temperatures.

Gold activation measurement

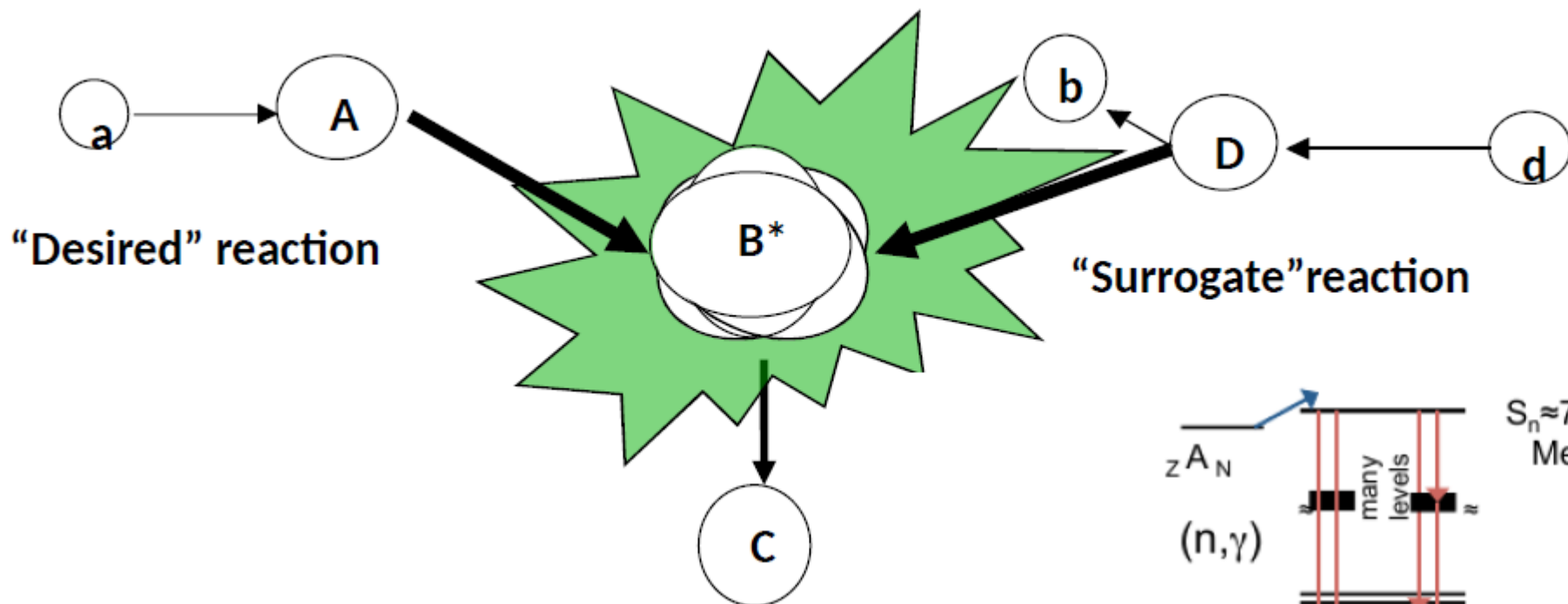
Irradiating a sample (sandwiched between two Au foils) to measure the MACS respect to the Au

Reference measurement
MACS of gold (Au-197)
(absolute measurement committed by IAEA)

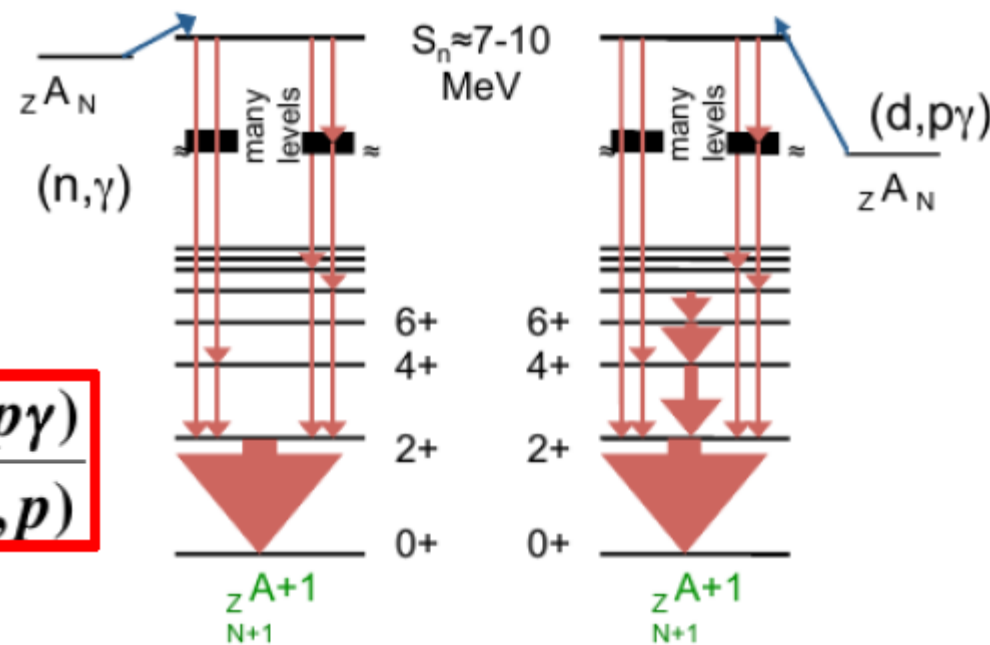
Benchmark measurement
MACS of yttrium (Y-89) or zirconium (Zr-94)

Well measured MACS
Moreover, the same reaction will be done at **CERN n_TOF irradiation facility** for comparison

Neutron capture cross sections via surrogate reaction approach



Also $^3\text{He}, ^4\text{He}$



$$\sigma_{n\gamma}^{WE}(E_n) = \sigma_n^{CN}(E_n) G_\gamma^{CN}(E_n) = \sigma_n^{CN}(E_n) \frac{N(d, p\gamma)}{\epsilon N(d, p)}$$

Neutron capture cross sections via surrogate reaction approach

What we measure:

$$P(d, pg) = \hat{\sigma}_{J,p} S_{(d,p)}(E, J, p) * G(E, J, p, g)$$

Entry state correction:
spin-parity distribution
needed!!

Decay of the
formed
compound
nucleus
(can be calculated)

What we want:

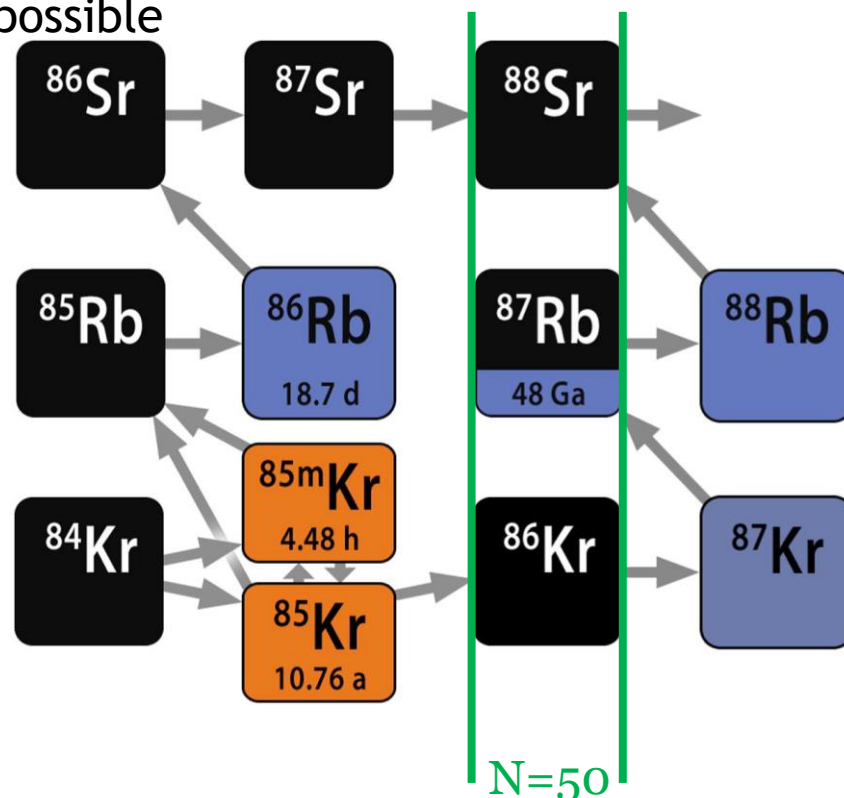
$$P(n, g) = \hat{\sigma}_{J,p} S_{(n,g)}(E, J, p) * G(E, J, p, g)$$

$^{85}\text{Kr}(d,p)$ w/ $E_x=10$ MeV, just above S_n

^{85}Kr branching

$$\sigma(^{85}\text{Kr}) = (55 \pm 45) \text{ mb}$$

When $\tau_\beta \sim \tau_n \rightarrow$ several paths are possible



- ✓ The branching is important for Rb and Sr abundances
- ✓ It offers an estimation of the neutron density
- ✓ Crucial for both main and weak component
- ✓ **Challenge present understanding!**

When ^{22}Ne neutron source is active

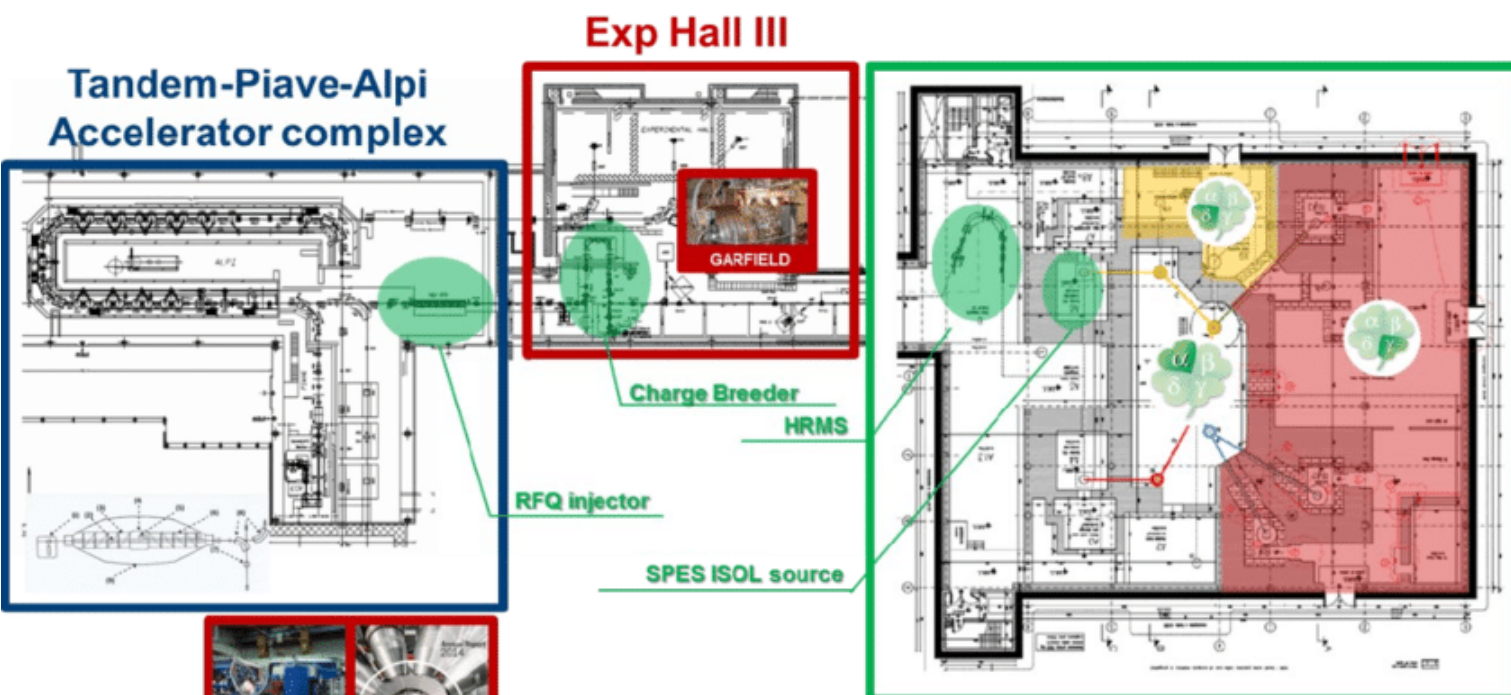
At high neutron densities ($5 \times 10^8 \text{ n/cm}^3$), about the 80% of the flux goes through ^{85}Kr , allowing the production of ^{86}Kr and ^{87}Rb :

--> ^{87}Rb in AGB stars is an indicator of the neutron density!

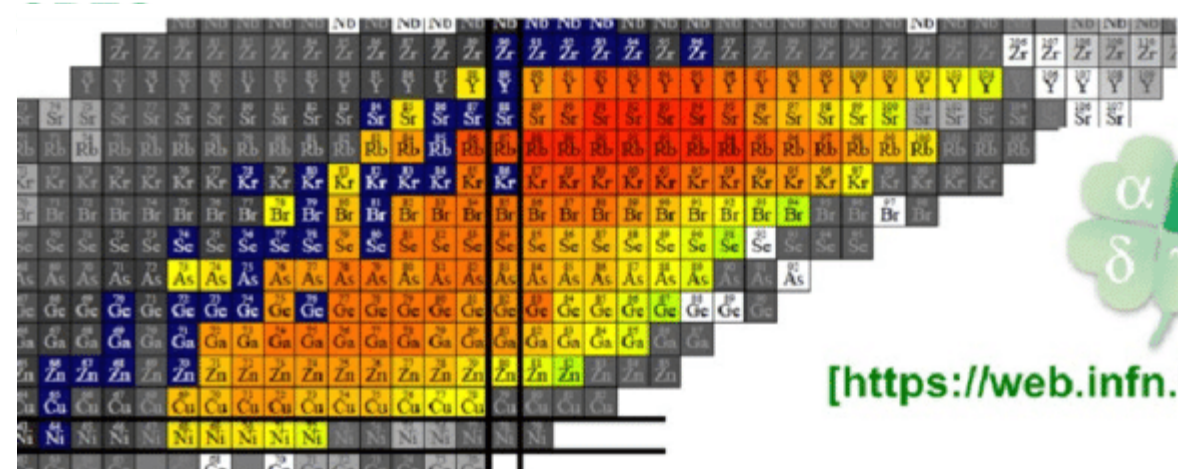
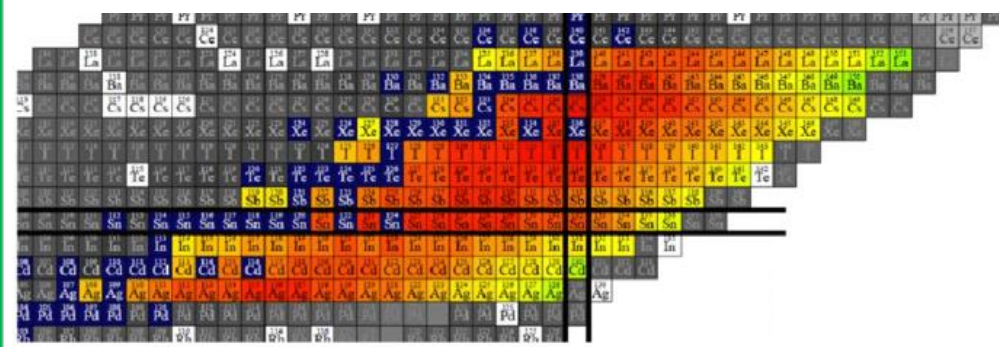
^{86}Kr , ^{87}Rb , and ^{88}Sr are all magic, with low neutron capture cross sections

- ✓ In low-mass stars: ^{88}Sr produced
- ✓ In massive AGB: ^{87}Rb

SPES reaccelerated beams

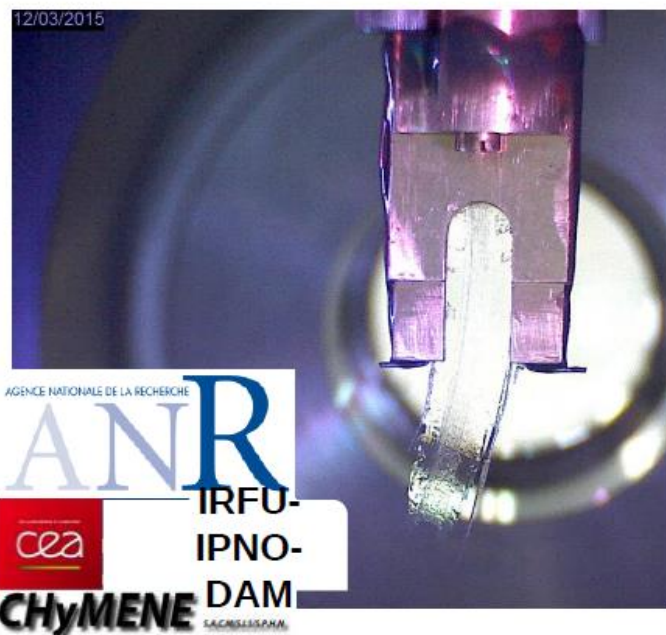


Exp Halls I and II



[<https://web.infn.it/spes/>]

Targets



- Hydrogen (h,d) target in a solid phase near triple point ($\sim 17\text{K}$)
- Thickness 50 – 200 μm
- No window - C free
- Continuous flow in vacuum 2-10mm/sec
- Compatible with particle detection



- H, D, ^3He , ^4He
- Dense: up to $\sim 10^{21}$ nuclei/ cm^2
- Havar window
- Compatible with particle det.

CTADIR
PRIN Giovani
A.Gottardo et al.

Neutron capture cross sections via surrogate reaction approach

s process

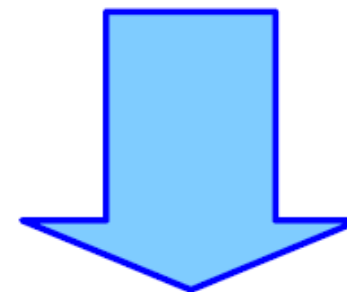
- (n,γ):
 - ^{79}Se , $^{81,85}\text{Kr}$, ^{86}Rb , ^{65}Zn , ^{121}Sn ,
 - ^{64}Cu , ^{108}Ag , ^{109}Pd , and ^{123}Sn and many more



- collaboration with INFN Pg and INAF Teramo
- 2 Lols presented at the 3rd SPES workshop in 2016
- Tests proposed at LNL

r process

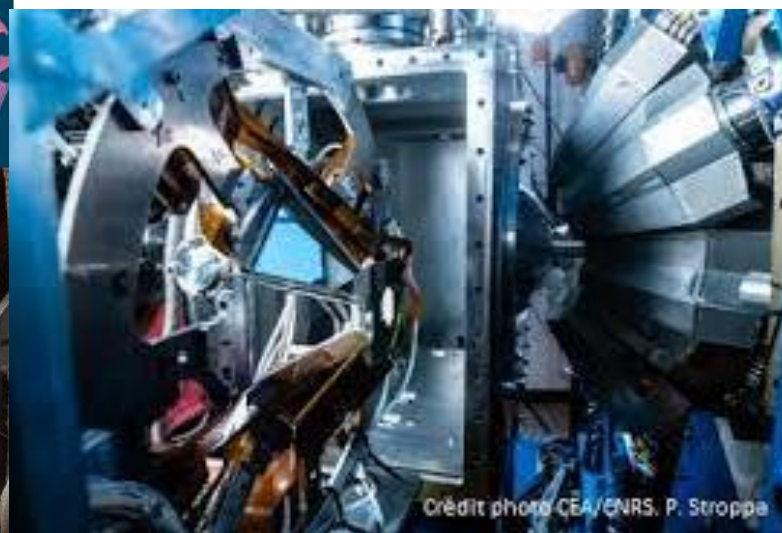
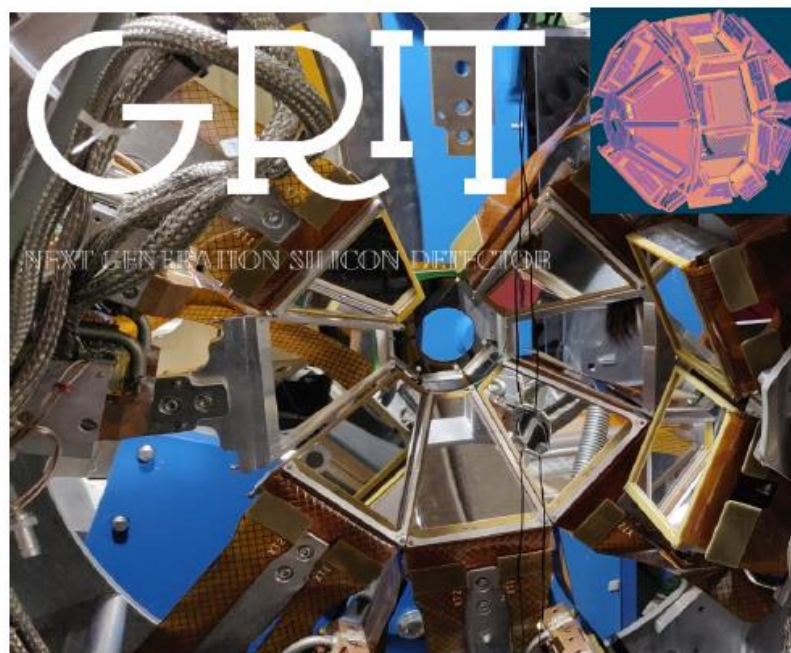
- $^{123,131-134,131}\text{In}$, ^{133}Sb
- Ni, Cu, Zn, Ga, Ge, As



- Collaboration with ORNL/Rutgers Univ. (exp) and NSCL (theory)
- 2 Lols presented at the 3rd SPES workshop in 2016
- Commissioning tests needed with stable beam

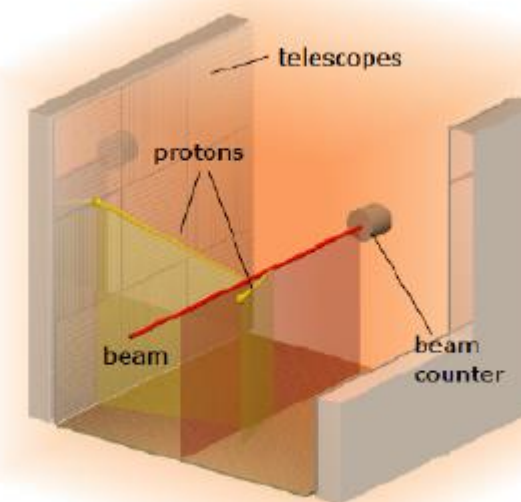
Instrumentation

**Traditional gamma/particle spectroscopy
but state-of-the-art tech.**



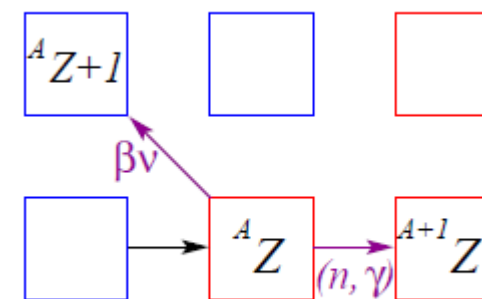
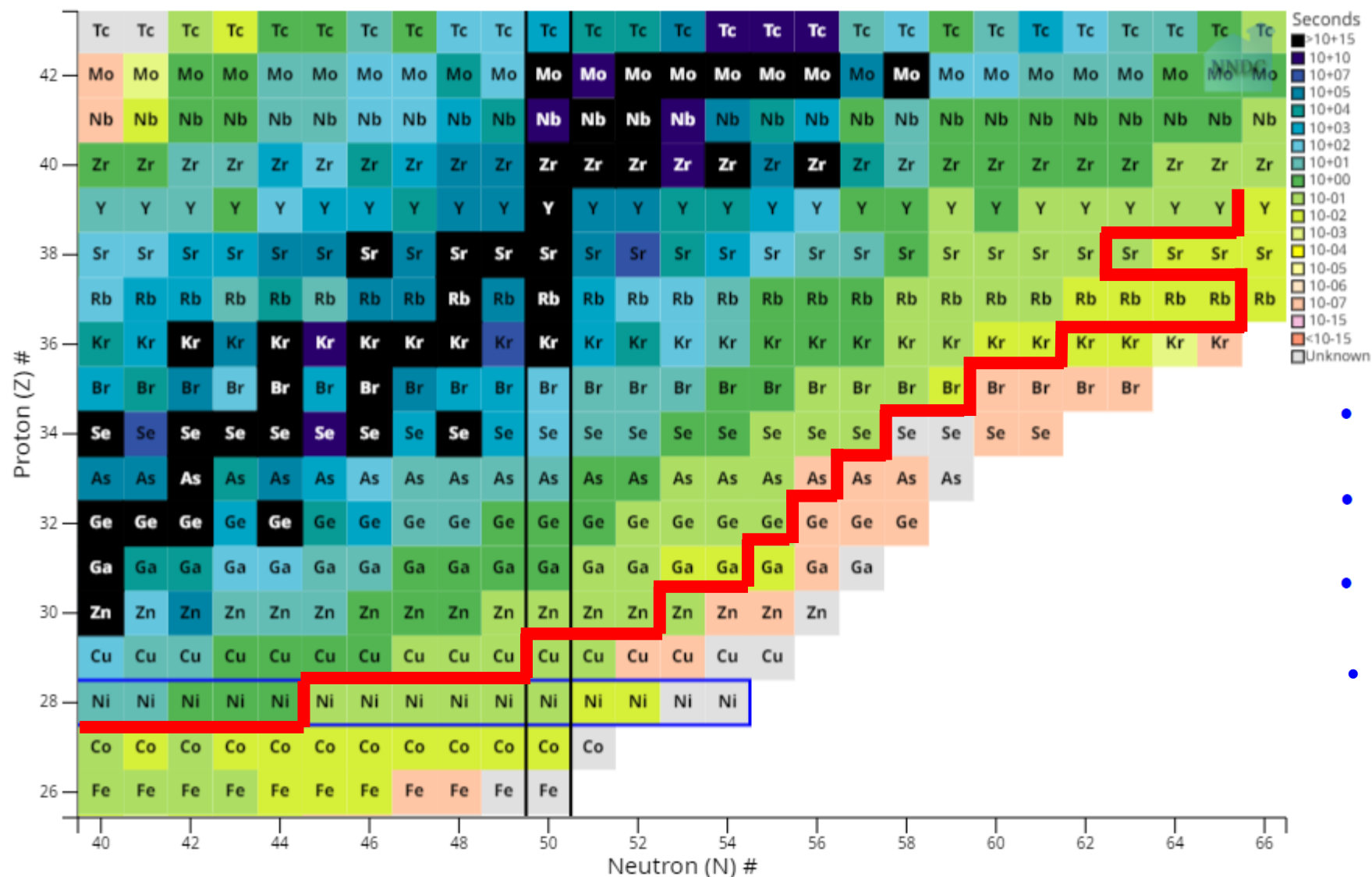
ACTAR-TPC + ANCILLARY DETECTORS

- Si-CsI telescope
- LaBr₃/CeBr₃ for γ -tagging



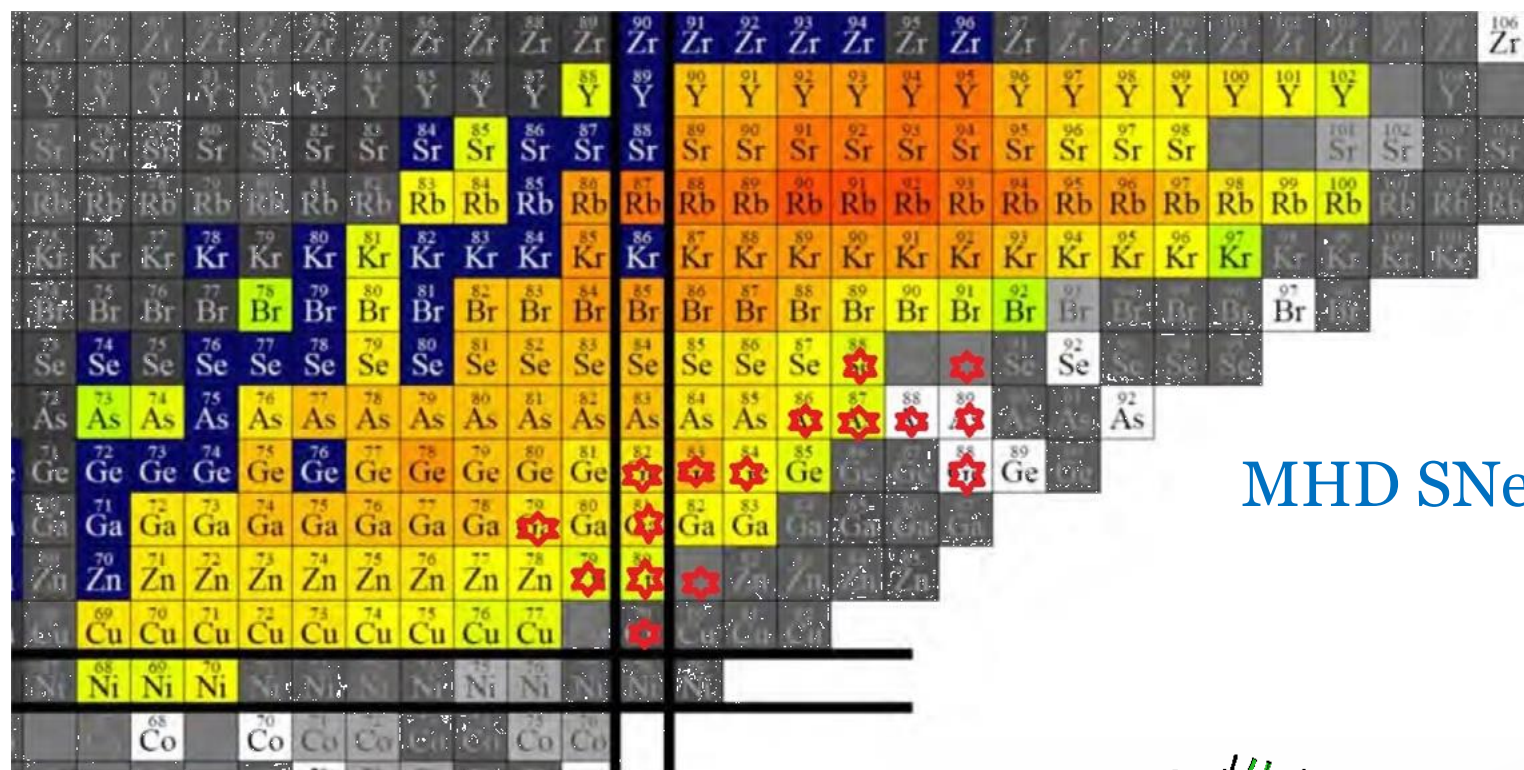
PHASE B/C

Experimental nuclear data



- beta decay rates
- Beta-delayed neutron emission
- neutron capture rates
- $(\alpha, n) \quad n-1 \xrightleftharpoons[\beta_n]{\alpha_n} n$

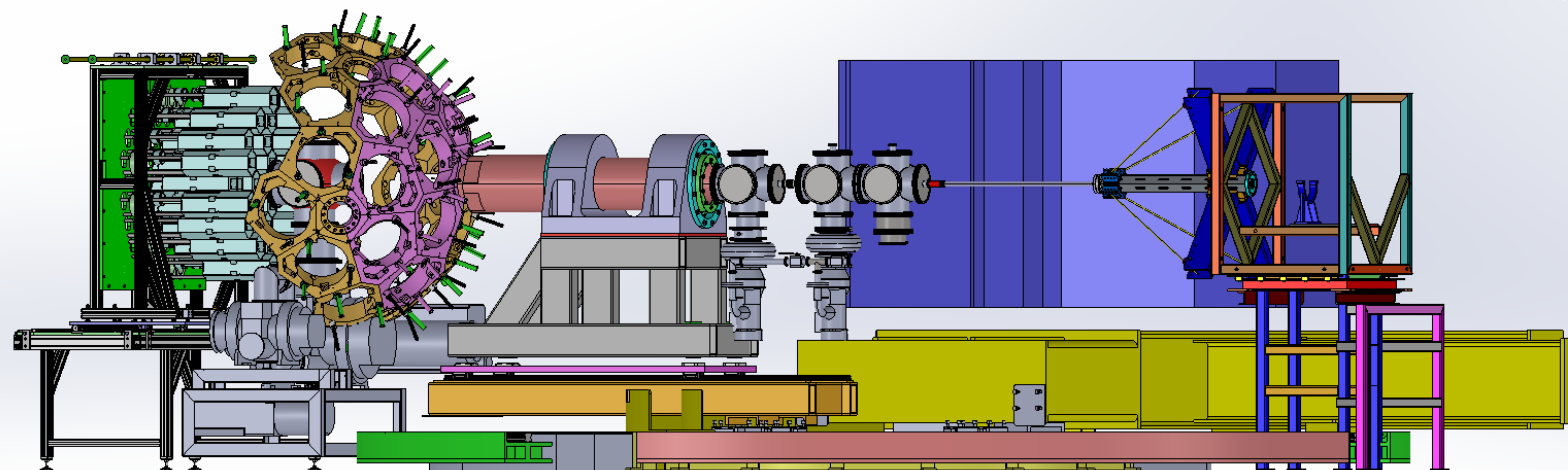
(α, n) reactions with reaccelerated SPES beams and SUGAR



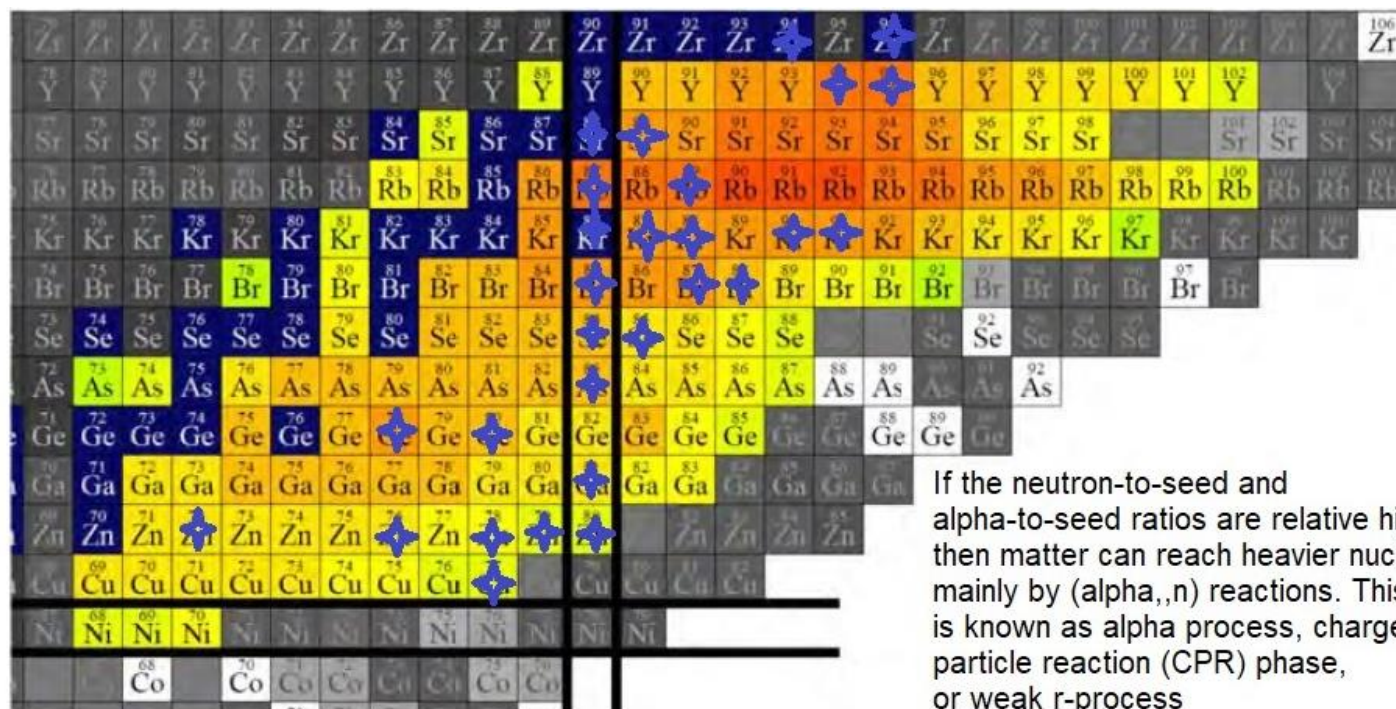
THE ASTROPHYSICAL JOURNAL, 927:116 (8pp), 2022 March 1

Table 1
Reaction Rate Variations That Affect Most Elements

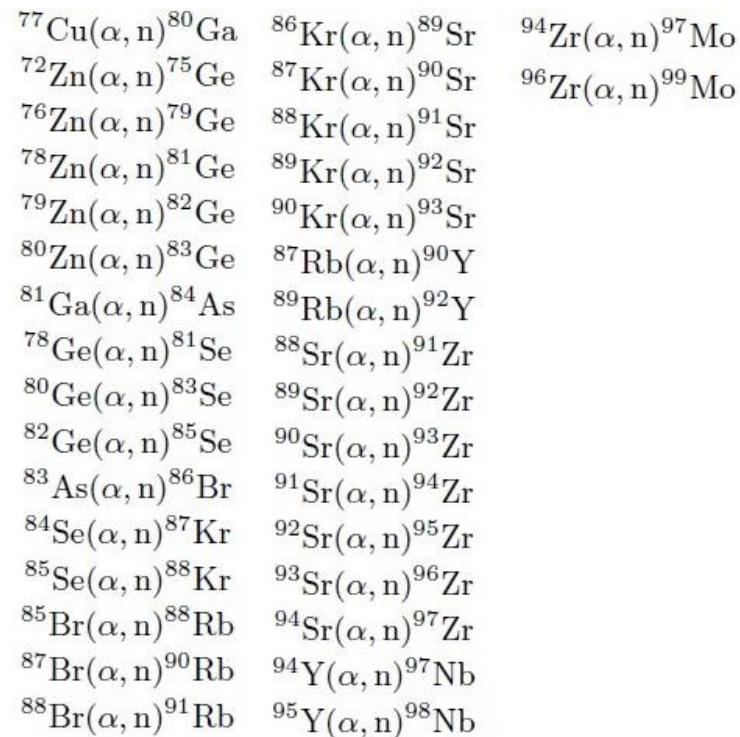
| Reaction | Z of Element | Tracer |
|-----------------------------|-----------------------------|------------|
| $^{80}\text{Zn}(\alpha, n)$ | 25–28, 33–52 | 1, 2, 3, 6 |
| $^{79}\text{Zn}(\alpha, n)$ | 25–27, 34–52 | 1, 2, 3, 6 |
| $^{81}\text{Zn}(\alpha, n)$ | 25–28, 34–46, 48–52 | 2, 3 |
| $^{81}\text{Ga}(\alpha, n)$ | 25–28, 34–45, 47, 48, 50–52 | 2, 8 |
| $^{79}\text{Cu}(\alpha, n)$ | 25–29, 52–66 | 2, 4 |
| $^{82}\text{Ge}(\alpha, n)$ | 25–27, 42–52 | 2, 8 |
| $^{83}\text{Ge}(\alpha, n)$ | 25–28, 44–52 | 2, 8 |
| $^{88}\text{As}(\alpha, n)$ | 25–29, 33–39 | 2 |
| $^{87}\text{As}(\alpha, n)$ | 25–29, 33–38 | 2 |
| $^{84}\text{Ge}(\alpha, n)$ | 26–29, 32, 33, 50–52 | 2, 8 |
| $^{79}\text{Ga}(\alpha, n)$ | 44–52 | 8 |
| $^{88}\text{Se}(\alpha, n)$ | 25–27, 34–39 | 2 |
| $^{90}\text{Se}(\alpha, n)$ | 25–27, 34, 36–39 | 2 |
| $^{86}\text{As}(\alpha, n)$ | 25–28, 35, 36, 38 | 2 |
| $^{78}\text{Ni}(\alpha, n)$ | 25–29 | 2, 3 |
| $^{86}\text{Ge}(\alpha, n)$ | 25–29, 32 | 2 |
| $^{89}\text{As}(\alpha, n)$ | 25–28, 33, 35 | 2 |



(α, n) reactions with reaccelerated SPES beams and SUGAR



If the neutron-to-seed and alpha-to-seed ratios are relative high then matter can reach heavier nuclei mainly by (α, n) reactions. This is known as alpha process, charged-particle reaction (CPR) phase, or weak r-process



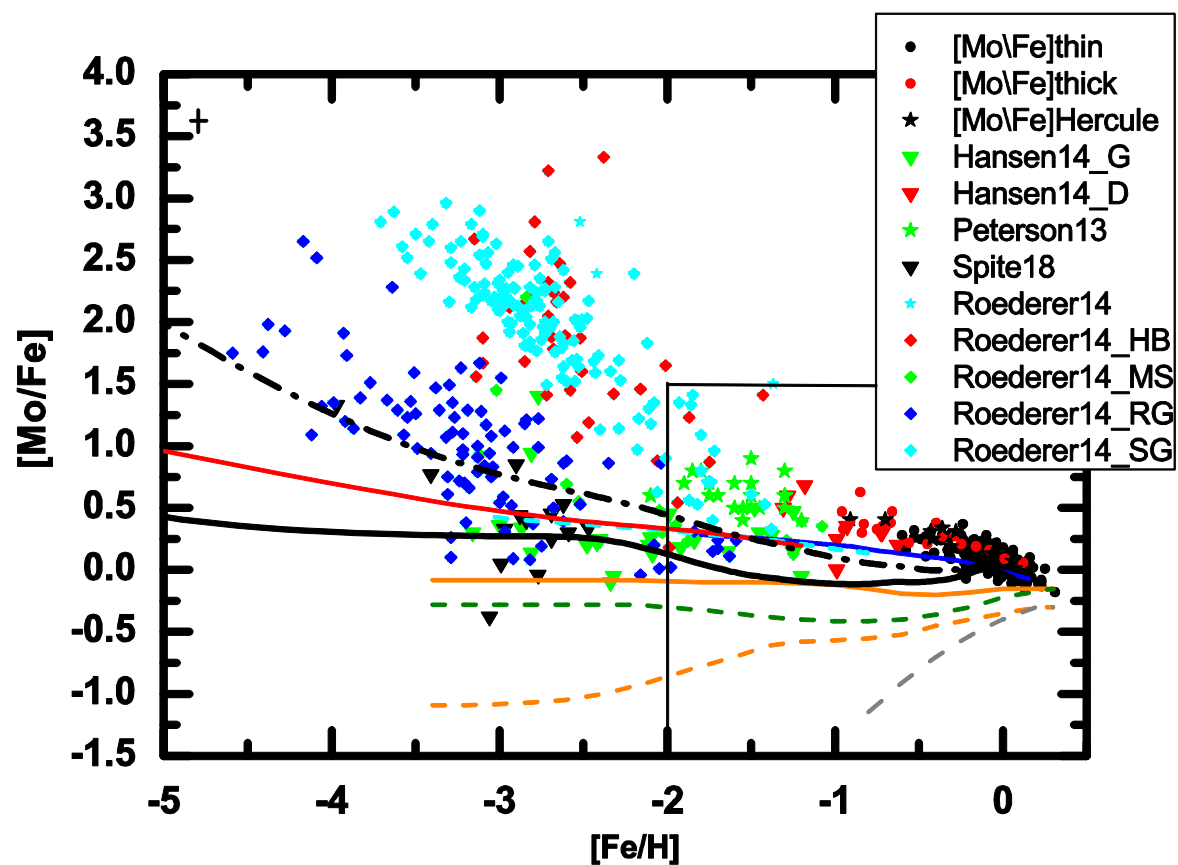
J. Bliss et al., Journal of Physics G: Nuclear and Particle Physics **44**, 054003 (2017)

TALYS 1.6 considered 909 (α, n) reactions on stable and neutron-rich nuclei between Fe ($Z=26$) and Rh ($Z=45$).

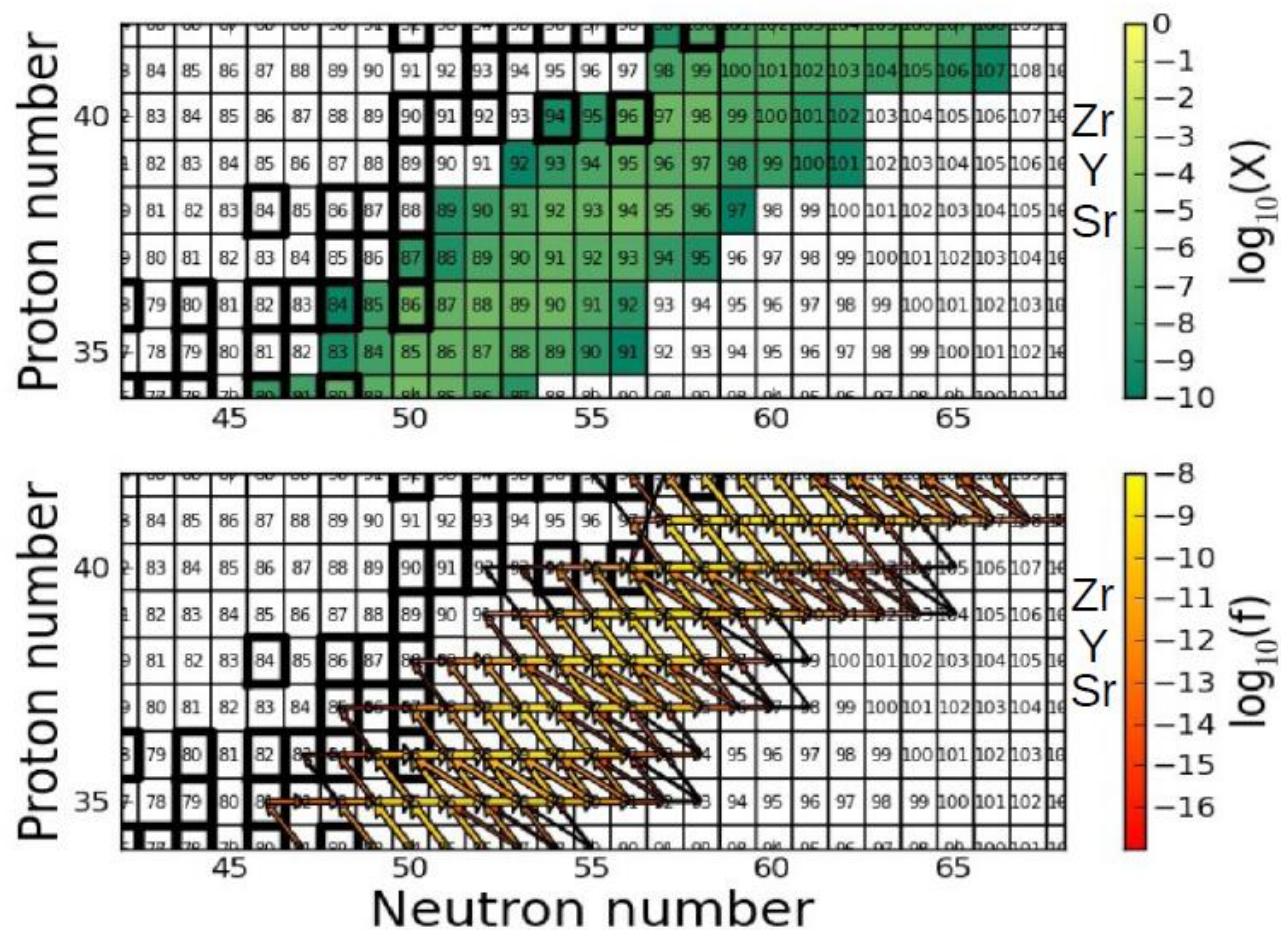
masses, which were taken from data table if available, or from the FRDM otherwise.

$$1 \text{ GK} \lesssim T \lesssim 5 \text{ GK}$$

The production of molybdenum in stars: a nuclear astrophysics challenge



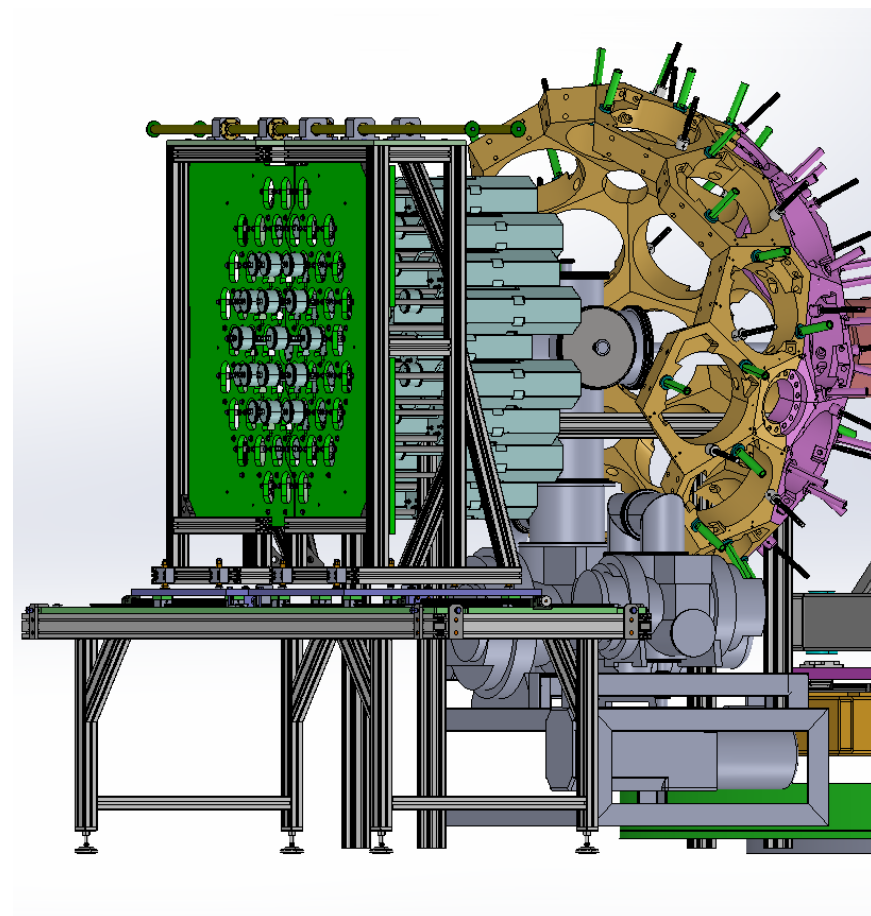
Nucleosynthesis properties of the i process: Se-Nb



The production of molybdenum in MHD SNe

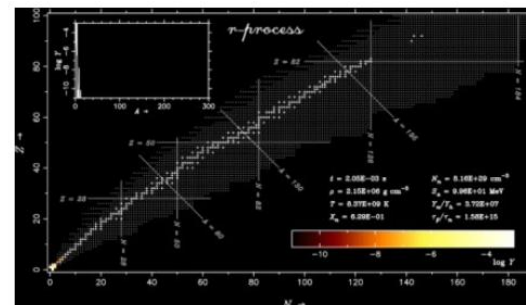
| Element | Reaction | Rate varied | $R(i)$ | Tracer |
|------------------------------|------------------------------|-------------|---------------------|---------|
| Mo ($Z = 42$) | $^{80}\text{Zn}(\alpha, n)$ | 100 | 0.326, 0.224, 0.099 | 3, 6, 1 |
| | $^{81}\text{Ga}(\alpha, n)$ | 100 | 0.234, 0.034 | 8, 3 |
| | $^{82}\text{Ge}(\alpha, n)$ | 100, 0.01 | 0.108, 0.110 | 8 |
| | $^{79}\text{Zn}(\alpha, n)$ | 100 | 0.195, 0.149, 0.066 | 3, 6, 1 |
| | $^{78}\text{Zn}(\alpha, n)$ | 100 | 0.173, 124 | 3, 6 |
| | $^{81}\text{Zn}(\alpha, n)$ | 100 | 0.119, 106, 0, 063 | 3, 6, 1 |
| | $^{83}\text{Ge}(\alpha, n)$ | 100 | 0.094 | 8 |
| | $^{79}\text{Ga}(\alpha, n)$ | 100 | 0.086 | 8 |
| | $^{80}\text{Ga}(\alpha, n)$ | 100 | 0.072 | 8 |
| | $^{81}\text{Ge}(\alpha, n)$ | 100 | 0.059 | 8 |
| | $^{90}\text{Se}(\alpha, n)$ | 100 | 0.049 | 2 |
| | $^{87}\text{As}(\alpha, n)$ | 100 | 0.045 | 2 |
| | $^{88}\text{Se}(\alpha, n)$ | 100 | 0.028 | 2 |
| | $^{121}\text{Tc}(\alpha, n)$ | 100 | 0.020 | 6 |
| | $^{119}\text{Tc}(\alpha, n)$ | 100 | 0.018 | 6 |
| | $^{89}\text{Nb}(\alpha, n)$ | 0.01 | 0.016 | 6 |
| | $^{103}\text{Nb}(\alpha, n)$ | 0.01 | 0.011 | 6 |
| $^{103}\text{Mo}(\alpha, n)$ | 100 | 0.010 | 6 | |

SUGAR@LNL coupled with NEDA



¹²C PRODUCTION IN EXPLOSIVE SCENARIOS

r-process escenario



¹²C is the seed nucleus for the creation of heavier nuclei (A=50-80)

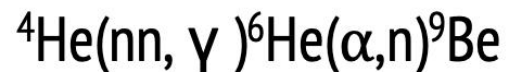
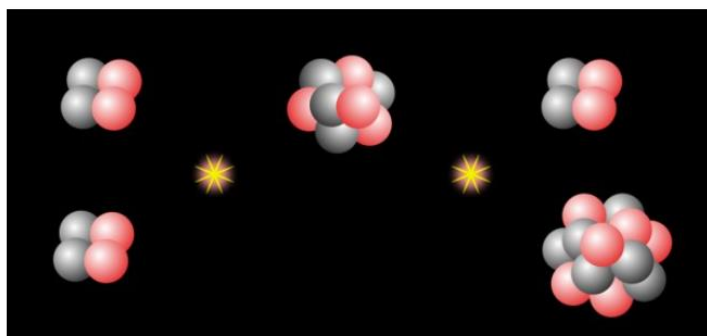
¹²C formation

Binary system of two neutron stars. Site where r-process can take place



E. Pian et al, Nature 551, 67–70 (2017)

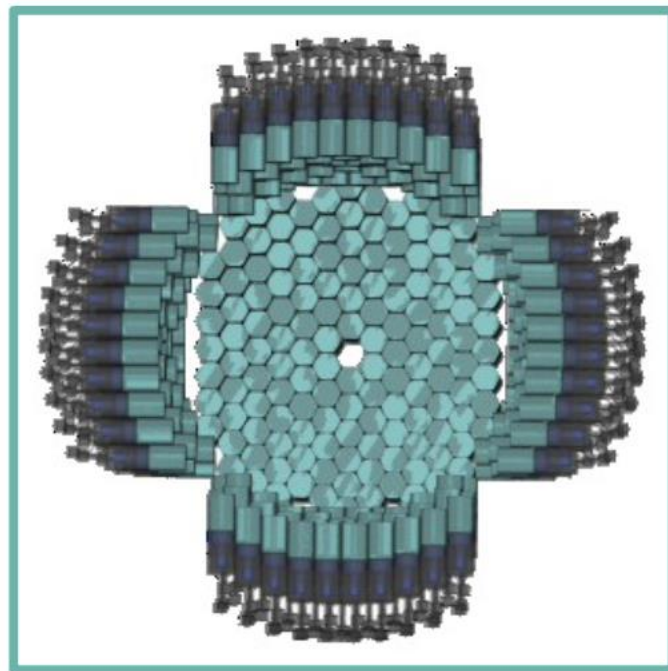
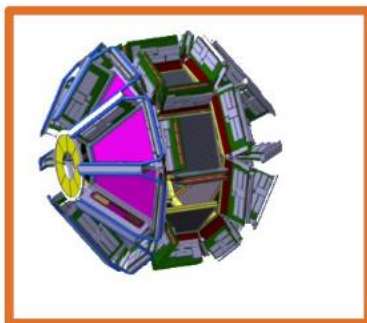
Triple alpha process



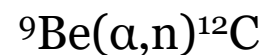
Favored by a factor ~10



- **Direct kinematic.** ${}^9\text{Be}$ target.
 - For instance: detector **GRIT (charged particles)** and **NEDA (neutrons)** .
Possible coincidence n - ${}^{12}\text{C}$



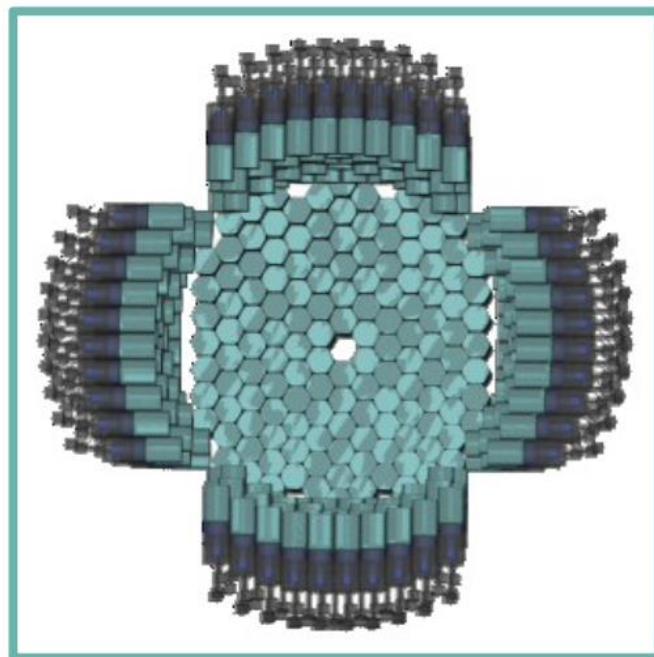
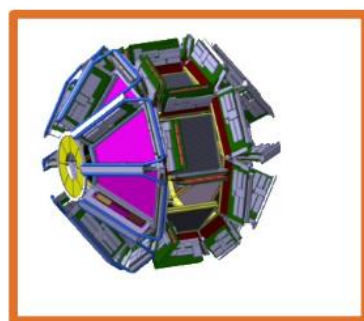
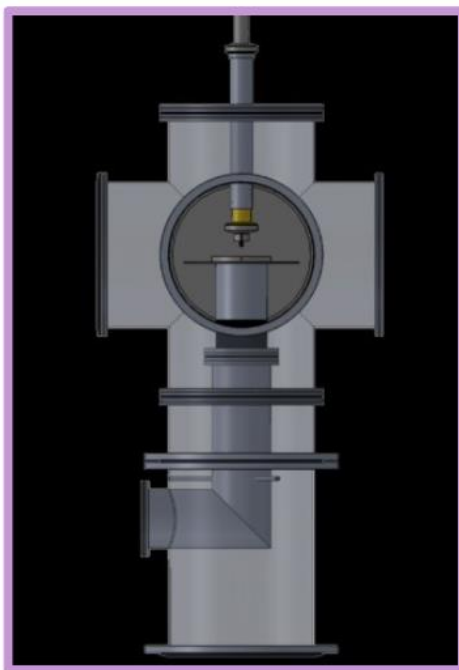
- $\alpha + \alpha + \alpha + n$
 $Q = -1.57 \text{ MeV}$
- ${}^8\text{Be} + n + \alpha$
 $Q = -1.66 \text{ MeV}$
- ${}^5\text{He} + 2\alpha$
 $Q = -2.31 \text{ MeV}$



- **Inverse kinematic.** ${}^4\text{He}$ target.
 - Gas target (CTADIR or **SUGAR**)
 - For instance: detector **GRIT (charged particles)** and **NEDA (neutron)**.

${}^9\text{Be}$ beam at LNL???

Possible coincidence n - ${}^{12}\text{C}$



- $\alpha + \alpha + \alpha + n$
Q = -1.57 MeV
- ${}^8\text{Be} + n + \alpha$
Q = -1.66 MeV
- ${}^5\text{He} + 2\alpha$
Q = -2.31 MeV

${}^4\text{He}(n,n,\gamma){}^6\text{He}$

- **Inclusive Coulomb breakup of ${}^6\text{He}$ on heavy target** \longrightarrow **Reaction rate ${}^4\text{He}(n,n,\gamma){}^6\text{He}$**

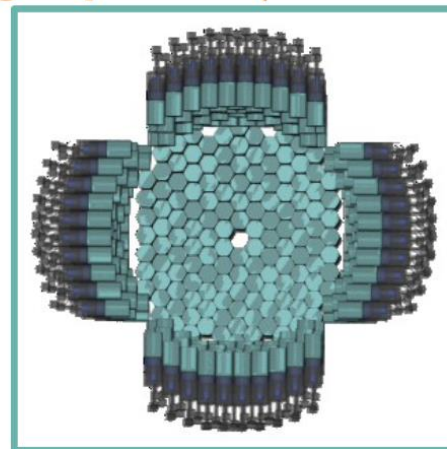
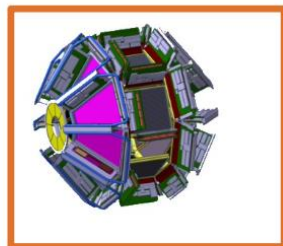
J. Casal et al., Phys. Rev C 93 (2016) 041602(R);

For instance: detector **GRIT (charged particles)**

- **Exclusive breakup measurements ${}^6\text{He}+A$**

For instance: detector **GRIT (charged particles)** and **NEDA (neutrons)**.

Possible coincidence n - ${}^4\text{He}$



- **Study the reaction ${}^6\text{He}({}^4\text{He},\gamma){}^{10}\text{Be}$**

The ${}^6\text{He}+{}^4\text{He}$ cluster structure of ${}^{10}\text{Be}$ is under study at the LNS with a ${}^{10}\text{Be}$ beam

For instance: detector **AGATA (gamma)**

Gas target (CTADIR or SUGAR)

${}^6\text{He}({}^4\text{He},\gamma){}^{10}\text{Be}$ $Q= 7.4$ MeV

${}^6\text{He}({}^4\text{He},n){}^9\text{Be}$ $Q= 0.6$ MeV

SUMMARY

- ✓ Decay properties of neutron-rich nuclei at the first and second r-process peak : $T_{1/2}$, Pn, decay schemes

- ✓ Neutron capture cross sections :
 - ✓ s-process : activation measurements and surrogate reaction approach
 - ✓ i-and r-process nucleosynthesis via surrogate reaction approach

- ✓ Abundances of the elements at the first r-process peak: (α ,n) reactions

- ✓ R-process seeds: ${}^9\text{Be}(\alpha, n){}^{12}\text{C}$; ${}^4\text{He}(2n, \gamma){}^6\text{He}$

For a very long term: fission of heavy neutron-rich
Separator able to cope with overlapping A/q

Extra

A decorative horizontal line consisting of a solid blue bar on top, followed by a white bar, and then a series of three thin blue lines on the right side.

Measurement of the ^{134}Cs excited state at 60.03 keV, whose SPIN is not known: it is currently identified as (3)+.

It may be 3+, 4+ or 5+.

- Population via b-decay not viable
- Access via different technique
- MOS technique could help accessing low-energy state
- Dedicated set of magnets for low-energy electrons transport
- Colling of Si(Li) might not be needed

| | | | | | |
|---|---|---|---|---|--|
| ^{134}Ba 51 y 0.00% | ^{134}Ba STABLE 2.417% | ^{135}Ba STABLE 6.592% | ^{136}Ba STABLE 7.854% | ^{137}Ba STABLE 11.232% | ^{138}Ba STABLE 71.698% |
| ^{132}Cs 30 d 0.13% 0.87% | ^{133}Cs STABLE 100% | ^{134}Cs 2.0652 y $\beta = 100.00\%$ $\epsilon = 3.0E-4\%$ | ^{135}Cs 2.3E+6 y $\beta = 100.00\%$ | ^{136}Cs 13.04 d $\beta = 100.00\%$ | ^{137}Cs 30.08 y $\beta = 100.00\%$ |
| ^{132}Xe STABLE 32% | ^{132}Xe STABLE 26.9086% | ^{133}Xe 5.2475 d $\beta = 100.00\%$ | ^{134}Xe > 5.8E+22 y 10.4357% 2β | ^{135}Xe 9.14 h $\beta = 100.00\%$ | ^{136}Xe > 2.4E+21 y 8.8573% 2β |
| ^{131}I 8.0252 h 0.00% | ^{131}I 8.0252 d $\beta = 100.00\%$ | ^{132}I 2.295 h $\beta = 100.00\%$ | ^{133}I 20.83 h $\beta = 100.00\%$ | ^{134}I 52.5 m $\beta = 100.00\%$ | ^{135}I 6.58 h $\beta = 100.00\%$ |

The beta-decay rate in astrophysical plasmas may change depending on the spin of that state, even at relatively low temperatures.

Possible measurement from

$^{134}\text{Xe} + ^{208}\text{Pb}$

or

$^{133}\text{Cs}(d,p)$ beams?

